Environmental Health Perspectives
Vol. 56, pp. 163-183, 1984

New Techniques for Imaging and Analyzing Lung Tissue

by Victor L. Roggli,* Peter Ingram,† Richard W. Linton,‡ William F. Gutknecht,† Pat Mastin,* and John D. Shelburne*

The recent technological revolution in the field of imaging techniques has provided pathologists and toxicologists with an expanding repertoire of analytical techniques for studying the interaction between the lung and the various exogenous materials to which it is exposed. Analytical problems requiring elemental sensitivity or specificity beyond the range of that offered by conventional scanning electron microscopy and energy dispersive X-ray analysis are particularly appropriate for the application of these newer techniques. Electron energy loss spectrometry, Auger electron spectroscopy, secondary ion mass spectrometry, and laser microprobe mass analysis each offer unique advantages in this regard, but also possess their own limitations and disadvantages. Diffraction techniques provide crystalline structural information available through no other means. Bulk chemical techniques provide useful cross-checks on the data obtained by microanalytical approaches. It is the purpose of this review to summarize the methodology of these techniques, acknowledge situations in which they have been used in addressing problems in pulmonary toxicology, and comment on the relative advantages and disadvantages of each approach. It is necessary for an investigator to weigh each of these factors when deciding which technique is best suited for any given analytical problem; often it is useful to employ a combination of two or more of the techniques discussed. It is anticipated that there will be increasing utilization of these technologies for problems in pulmonary toxicology in the decades to come.

Introduction

Increasing interest of the public sector and the scientific community in the effects of environmental pollutants and toxins on man has resulted in the application of new and ever more sophisticated analytical techniques and instrumentation to study the interaction of these pollutants with human tissues. The lung, which is constantly exposed to airborne particulate and gaseous species, is an ideal setting in which to study the various substances which contaminate the atmosphere and the manner in which they may produce tissue damage. The past few decades have witnessed a revolution in the field of imaging techniques at the microscopic level; some of these techniques, including scanning electron microscopy, transmission electron microscopy, backscattered electron imaging, and energy-dispersive X-ray analysis, have been discussed elsewhere in this volume. It is the purpose of this review to cover some additional techniques which have particular application in the study of pulmonary toxicology. Many of these techniques have in only a few instances been employed in the analysis of problems in environmentally related pulmonary diseases.

A brief summary of the techniques, instrumentation, and application of X-ray analytical methods, microprobe mass spectrometry, chemical analytical techniques, and electron microscopic approaches are the specific subjects of this discussion. Using various combinations of these techniques and appropriate sample preparation, it is possible to determine quantitatively or semiquantitatively the elemental or chemical composition of a specimen, and in some instances, to obtain (with varying degrees of spatial resolution depending on the techniques employed) an image of the specimen indicating the precise localization of the elements of interest. The applicability of such an approach to the identification of particulates in pulmonary tissues is readily apparent (Table 1). It is important that these techniques be standardized and the data generated with them compared to those available with conventional bulk chemical analyses. The latter have the advantages of greater sensitivity for most elements, ability to rapidly sample large amounts of tissue, and greater facility for empirical quantitation using standards. Many of the microscopic techniques to be described, on the

*The Department of Pathology, Duke University, and Veterans Administration Medical Center, Durham, NC 27710.

†Chemistry and Life Sciences Division and Energy, Engineering and Environmental Sciences Division, Research Triangle Institute, Research Triangle Park, NC 27709.

‡Department of Chemistry, University of North Carolina, Chapel Hill, NC 27514.

Table 1. Application of selected techniques for analysis of lung tissues and cells: potential applicability for analyzing lung tissues and cells.

Technique (Abbr.)	Technique	Scope	References
Microanalytic techniques			
TRIX	Total rate imaging with X-rays	Identification and localization of inorganic particulates in organic matrix	(*1–3*)
AES, SAM	Auger electron spectroscopy, scanning auger microprobe	Detection and measurement of lighter elements ($Z < 9$) in tissues and cells; surface analysis of particles/cells	(*4–9*)
EELS	Electron energy loss spectrometry	Detection and measurement of lighter elements ($Z < 9$) in tissues and cells in very small spatial volume	(*10–12*)
SIMS	Secondary ion mass spectrometry, ion microprobe or microanalyzer	Analysis and 3-D mapping of elements in particles, cells and tissues at ppm levels with broad elemental coverage	(*1,8,13–17*)
LAMMA	Laser microprobe mass analyzer	Analysis of particles, cells and tissues at ppm level with broad elemental coverage	(*18–22*)
SAED	Selected area electron diffraction	Determination of crystalline structure of inorganic particulates (or organic crystals) in cells and tissues	(*23–29*)
Macroanalytic (bulk) techniques			
XRD	X-ray diffraction	Determination of crystalline structure of inorganic particulates extracted from cells or tissues	(*30–34*)
XRF	X-ray fluorescence	Detection and measurement of elements ($Z \geq 9$) extracted from cells or tissues	(*7,35*)
PIXEA	Proton-induced X-ray emission analysis	Detection and measurement of elements ($Z \geq 9$) within organic matrix	(*3,36–38*)
AAS	Atomic absorption spectrometry	Trace analysis of metals isolated from tissue or cell extracts	(*39–41*)
ICP-AES	Inductively coupled plasma atomic emission spectroscopy	Trace analysis of elements isolated from tissue or cell extracts	(*42–44*)
NAA	Neutron activation analysis	Trace analysis of elements within organic matrix and labeling particles for radioactive tracer studies	(*45–47*)

other hand, permit analysis of individual cells or microscopic particles, but have the disadvantages of sampling-error problems, length of time required to obtain data on a large number of particles, and the extensive sample preparation required for *in situ* biological microanalysis. For many problems in pulmonary toxicology, the ideal approach is a combination of both bulk and microanalytical techniques.

Electron Microscopic Techniques

Total Rate Imaging with X-Rays (TRIX)

Energy dispersive X-ray analysis (EDXA) is a technique which allows the investigator to determine the chemical composition of a minute portion of a specimen by use of an electron beam. As described by Brody (*48*), the finely focused electron beam interacts with the atoms in the area on which the beam is directed, dislodging electrons from lower energy levels. The inner shell vacancies are replaced by a cascade effect of higher energy electrons, with resultant emission of X-rays with energy (or wavelength) properties which are characteristic for the elemental composition of the portion of the sample bombarded by the electron beam. With an energy-dispersive spectrometer, the X-ray events are detected and their characteristic energy measured using a lithium-doped, silicon detector and a multichannel analyzer. Conventional energy dispersive X-ray analysis displays the information as a series of peaks indicative of the elements present from which elemental concentrations may sometimes be calculated (*1*).

In total rate imaging with X-rays (TRIX), an image is produced when all the X-ray events generated in the electron beam scanning process are synchronously displayed (*2*). This is accomplished by transmitting all the X-ray events recorded by the Si(Li) detector directly to the video amplifier and image display system of a scanning electron microscope. Detection is limited to those elements with an atomic number (Z) greater than or equal to 9. The similarity of this technique to dot maps of specific elements should be noted (*13*); the difference is that with TRIX, *all* the elements in a given area which have an atomic number within the sensitivity limits of the detector and which are present in sufficient quantity will collectively give rise to an image corresponding to the location of these elements within the specimen. Each X-ray event appears as a dot on the screen, and depending on the concentration of elements of a given atomic number, the pulses will pile up and

give rise to a gray-scale image which is dependent upon atomic number, topography, and orientation of the specimen. The image may be recorded using photographic film, which also serves to integrate the pulses or dots into a "continuous" image.

The greatest utility of TRIX is in detecting particulates or other constituents of relatively high atomic number within a matrix of lower atomic number (e.g., inorganic particulates within paraffin-embedded sections of lung tissue). Backscattered electron imaging (BEI) (*48*) may similarly be used to detect particulates of a high atomic number in a matrix or background of low atomic number (*49*). However, TRIX and BEI differ in several fundamental respects. First, the spatial resolution and depth of penetration of electrons and X-rays within a solid of low to moderate atomic number are substantially different (Fig. 1). The resolution for TRIX is at present somewhat better than 1 μm. Secondly, TRIX has completely different sensitivity characteristics with regard to increasing atomic number than conventional BEI techniques (Fig. 2). The total number of X-rays generated is a complex function of atomic number. This is because X-rays for *K*, *L*, and *M* shells (as well as continuum) must be summed to obtain total X-ray counts, and the efficiency of excitation of X-rays is different for *K*, *L*, and *M* shells for a given electron voltage. The advantages of BEI include its considerably greater detection efficiency and better spatial resolution. The advantages of TRIX include its increased sample depth response and minimization of

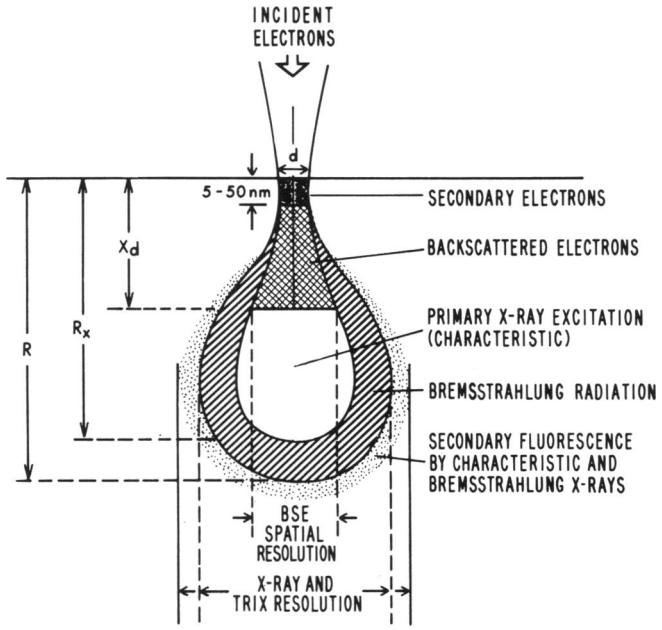

FIGURE 1. Penetration and resolution of X-rays vs. electrons within a solid of low to moderate atomic number (*Z*). *d* represents the diameter of the electron probe, X_d is the effective range for backscattered electrons, *R* is the total electron range, and *Rx* the effective X-ray range. The X-ray spatial resolution is a function of $(d + Rx)$. After Beaman and Isasi (*1*), from Ingram and Shelburne (*2*), with permission.

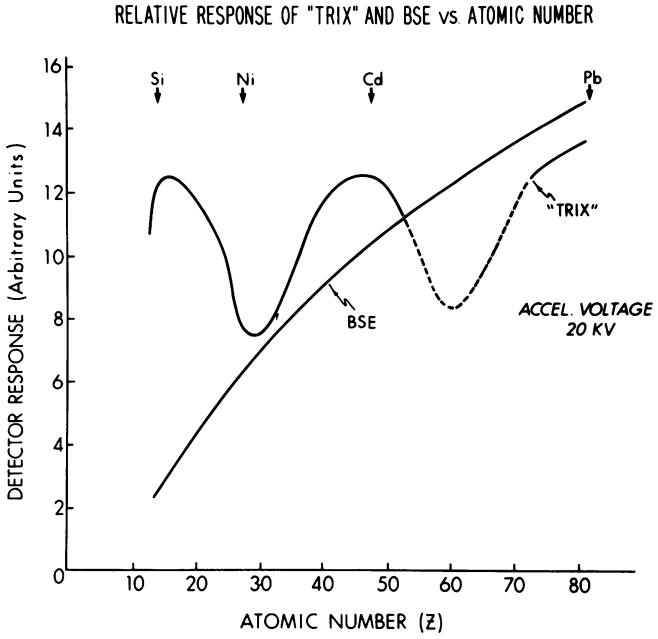

FIGURE 2. Relative response vs. atomic number of total rate-imaging with X-rays (TRIX) as compared to backscattered electron imaging. From Ingram and Shelburne (*2*), with permission.

the organic topographic matrix effects which may interfere with particle identification by BEI. Note that TRIX is particularly sensitive to silicon and aluminum, elements of importance in pulmonary toxicology. In practice, it is often beneficial to use both TRIX and BEI as complementary techniques.

We have used TRIX to study inorganic particulate content of human alveolar macrophages, tissue sections of individuals with pneumoconiosis, and cigarette smoke condensate (*50*). In each of these instances, the superior depth response of TRIX permitted identification of particles not detected or poorly resolved by BEI (*2*). An example is illustrated in Figure 3. TRIX may also be used to determine the optimal orientation of a specimen for energy dispersive X-ray analysis, avoiding topographical interferences between the region of interest and the detector. In addition, TRIX is of value in histochemical studies of cells in which it is desirable to correlate surface morphology with localization and quantitation of specifically stained organelles (e.g., dialyzed iron staining of small mucous granules in the tall mucous cells of the tracheal or bronchial epithelium) (*51*). Finally, in EDX analysis of mixed particulate samples, such as obtained from ambient air, water samples, or extracted from tissues, it is desirable to know which particles as seen in a scanning or backscattered image can give rise to a detectable EDX signal. TRIX may be used to specifically identify those particles containing elements which may give rise to EDX spectra; these particles may then be counted, analyzed for chemical composition by EDX analysis, and a particle size distribution obtained. A similar

approach to TRIX has been described by Legge and Hammond (*3*), in which X-rays are generated by a proton rather than electron source, and the X-ray events stored in a computer for future retrieval and analysis.

Auger Electron Spectroscopy (AES)

As discussed above, one result of the interaction of the electron beam with sample atoms is the ejection of inner shell electrons. The excess energy resulting from an outer shell electron filling a lower energy core vacancy is dissipated via either X-ray emission or the ejection of another outer shell electron, the Auger electron. The Auger electron possesses kinetic energy characteristic of the element of origin (*4*).

The Auger electron spectrometer (AES) consists of an electron gun, ultrahigh vacuum system, electron-energy analyzer and electron multiplier. The instrument is usually operated at a primary electron accelerating voltage of 0.5 to 10 KeV, with typical beam currents ranging from about 0.1 to 100 μamp. State-of-the-art electron energy analyzers with respect to optimum transmission and energy resolution are commonly of the cylindrical mirror design (*8,9*). An instrument permitting high lateral resolution analysis is the scanning Auger microprobe (SAM) in which a finely focused

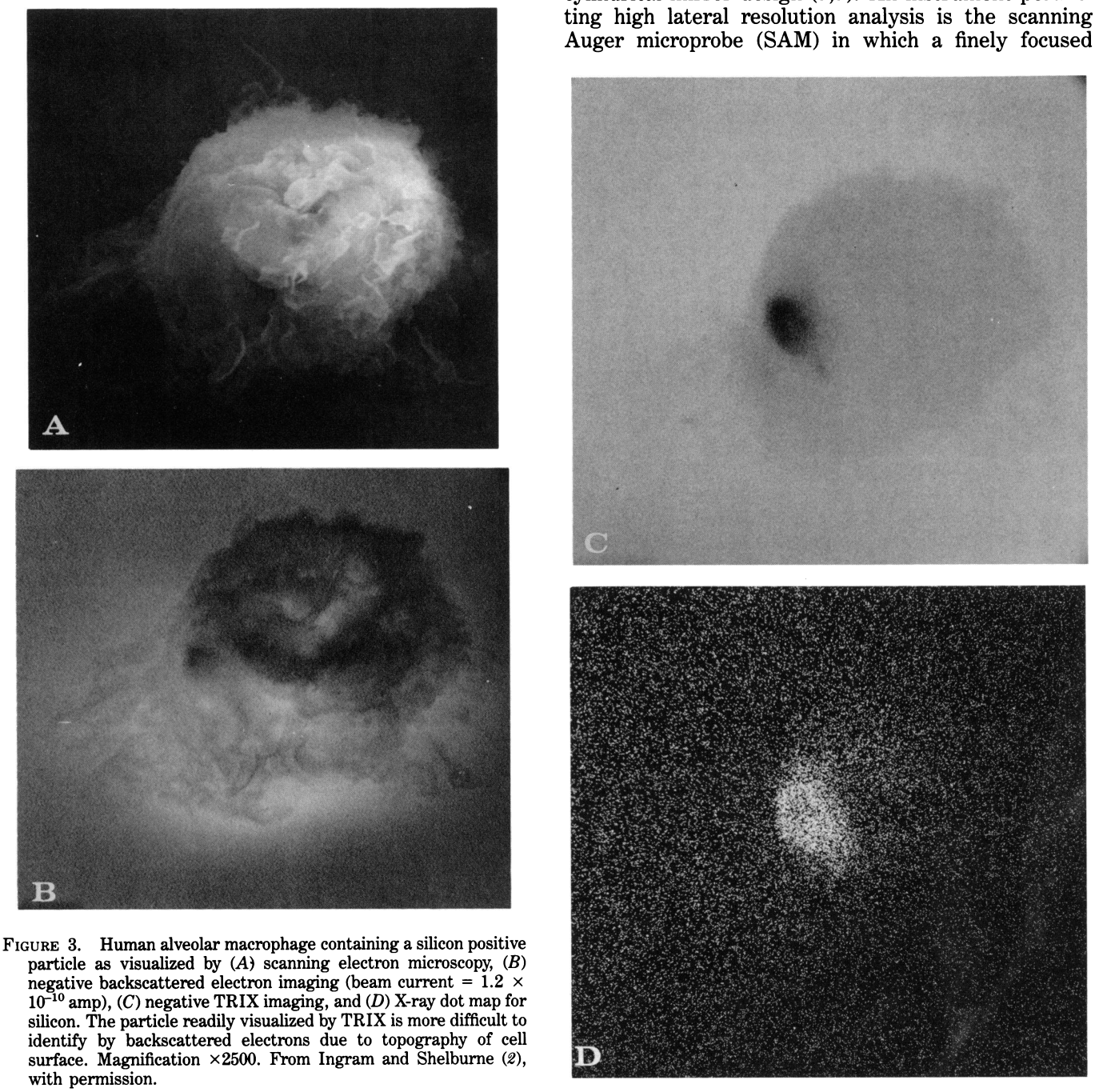

FIGURE 3. Human alveolar macrophage containing a silicon positive particle as visualized by (*A*) scanning electron microscopy, (*B*) negative backscattered electron imaging (beam current = 1.2×10^{-10} amp), (*C*) negative TRIX imaging, and (*D*) X-ray dot map for silicon. The particle readily visualized by TRIX is more difficult to identify by backscattered electrons due to topography of cell surface. Magnification ×2500. From Ingram and Shelburne (*2*), with permission.

electron beam is rastered across the surface of the specimen. The resultant Auger intensity for a given element may be converted into an elemental map in a manner analogous to dot maps obtained by EDXA. The minimum electron beam spot size and lateral resolution of Auger images is now approaching 50 nm. The minimum detection limit for AES is 2×10^9 atoms, and the minimum sample volume is 1×10^{-12} cm^3. The corresponding values for SAM are about 3×10^5 atoms and 2×10^{-17} cm^3 (*7*). Typical relative elemental detection limits are on the order of 0.1% atomic within the analytical volume.

Since Auger electron emission predominates over X-ray emission for low atomic number elements, Auger spectroscopy is more sensitive than EDXA for the detection of light elements (e.g., for $Z < 9$) (*5,7*). In addition, Auger elemental sensitivity remains relatively constant (within a factor of 10) as a function of atomic number, thus facilitating semiquantitative analyses. Because of the inelastic scattering of the low energy Auger electrons as they traverse the sample matrix, only those Auger electrons excited near the surface (typically < 100 Å) escape without energy loss to produce sharp spectral features superimposed on a slowly varying background of inelastically scattered electrons. Electrical charging of insulating particulate and biological specimens is of major concern, however, since the surface specificity of AES limits the utility of conducting surface films as used in conventional electron microscopy.

We have employed Auger electron spectroscopy to study the chemical composition of particles found in human alveolar macrophages. Macrophages obtained by bronchoalveolar lavage were treated with acid-base hydrolysis (4 N HCl followed by 1 N KOH in 50% ethyl alcohol over a steam bath for 24 hr), and the residue was mounted on a gold substrate. Scanning Auger microprobe analysis of individual particles demonstrated that these were mostly carbon (91.2% of the atoms present), with lesser amounts of oxygen, nitrogen, sodium, iron, sulfur, silicon and aluminum (*52*). Conventional EDXA studies showed weak X-ray emission for aluminum and silicon only, and electron diffraction studies had indicated that the carbon particles were noncrystalline.

Another application of Auger spectroscopy is in the study of toxic trace elements deposited on the surfaces of inorganic particulates in the respirable size range. Evidence for the concentration of toxic elements on the surface of particles derived from a variety of pollution sources is described elsewhere (*8*). Enhanced surface availability may result in enhanced bioavailability and thus is of potential interest in lung pathology. Although Auger analysis is limited to the outermost atomic layers of the specimen, most AES and SAM instruments are equipped with an ion sputtering gun, which permits etching away of successive surface layers, which may in turn be analyzed for chemical composition. Hence an in-depth chemical profile of isolated particles or of particles embedded in lung tissues may be obtained with this approach (*8*). A disadvantage of AES is the requirement of a very high vacuum in the sample chamber to reduce surface contamination, which can be a serious problem with this technique.

Electron Energy Loss Spectrometry (EELS)

The interaction of an electron beam with the atoms of a specimen results in electronic transitions characteristic of the elemental composition of the sample, as discussed above. These transitions also result in discrete energy losses by the inelastically scattered primary electrons which pass through the specimen. Analysis of the distribution of energy losses of these inelastically scattered electrons hence provides information concerning the elemental composition of the sample. The instrumentation for electron energy loss spectrometry (EELS) consists of a conventional or scanning transmission electron microscope equipped with an electron energy detector for separating electrons of different energies (e.g., a magnetic sector spectrometer) and a multi-channel analyzer. This analytical technique permits a high detection efficiency, since there is a concentration of forward scattering of the inelastically scattered electrons, whereas X-rays and Auger electrons are scattered to a first approximation isotropically (*10*). Spatial resolution of EELS is usually in the hundreds of Ångstroms, but can in principle be at the resolution of the microscope depending on the spectrometer configuration (*10*). The sensitivity of the technique potentially provides broad elemental coverage from lithium on through the periodic table.

Sample preparation requires the use of thin sections on the order of 0.1μ thick. Multiple inelastic and mixed elastic and inelastic interactions between the incident electrons and sample atoms occur with greater frequency as the sample thickness increases. This factor together with an increased background to peak signal ratio with greater sample thickness essentially limits the sample thickness to approximately one mean free path for inelastically scattered electrons (*10*). The high spatial resolution of EELS together with its sensitivity for lighter elements offer certain practical advantages in some problems in pulmonary toxicology. For example, Galle et al. (*11*) have used EELS in the analysis of beryllium particles as small as 0.01 μm in thin sections of lung tissue (calculated particle mass of 10^{-18} g). EELS involves full thickness analysis of the specimen, and in this sense may be considered complementary to Auger electron spectroscopy, which is primarily a surface analytical technique. Problems encountered with EELS include many interferences with the organic matrix (*11*) and for crystalline materials, interferences due to Bragg reflections of the diffracted incident electrons (See "Diffraction Techniques"). The latter problem when recognized can be resolved by tilting the specimen. EELS seems to have promising potential as an analytical technique in pulmonary toxicology, but

thus far few applications to the study of lung tissues and cells have been reported.

Diffraction Techniques

Selected Area Electron Diffraction (SAED)

When a crystalline substance is examined in any transmission electron microscope, a diffraction pattern forms in the back focal plane of the objective lens (*23*). Many transmission electron microscopes are designed so that the diffraction pattern may be focused in the image plane of the objective lens, hence forming a series of bright spots on the viewing screen. In practice, this is accomplished by weakening the first projector lens to increase its focal length. The distance R between the individual spots of the diffraction pattern and the central spot is related to the interplanar spacing d of the crystal by the formula, $Rd = n\lambda L$, where n is an integer, λ is the wavelength of the incident radiation in nanometers (approximately 0.004 nm for an electron beam at accelerating voltage of 80 kV), and L is the distance from the specimen to the photographic plate. The term λL, known as the camera constant, may be calculated from a standard of known and carefully characterized crystalline structure. Thus, the d interplanar spacings may be calculated by directly measuring the R values on a photograph of the diffraction pattern. The diffraction patterns of many thousands of known crystalline substances have been analyzed and catalogued in the ASTM index (*53*), so that the pattern of an unknown material may be compared with the indexed patterns for identification purposes. Obviously, if something is known of the chemical composition of the unknown material, the process of classification or indexing of the pattern will be greatly simplified.

Since the electrons which form the diffraction pattern are transmitted through the specimen, materials to be examined by electron diffraction must be very thin. Modern electron microscopes are designed such that an area of diameter of approximately 1 μm can be examined and a diffraction pattern obtained from individual particles, or from a selected portion of a larger particle or material. Hence, the process is termed selected area electron diffraction (SAED). Although electron diffraction patterns may be obtained from any inorganic crystalline particulate, much of the application of SAED techniques in the study of problems in pulmonary toxicology to date have dealt with the identification of asbestos in lung tissues (*26–29*). This is perhaps related to the distinctive and readily recognizable diffraction patterns produced by asbestos fibers (Fig. 4). Other investigators have used electron diffraction to study other inorganic particulates in the lung in various pneumoconioses (*24*), and this technique has also been applied in the identification of kaolinite in digests of lung tissue from cigarette smokers (*25*). SAED has perhaps its greatest utility as a complementary technique to energy dispersive spectrometry (EDXA), since many mineral species (e.g., the clay minerals) cannot be uniquely classified on the basis of elemental or chemical composition alone.

Disadvantages of SAED techniques are that the specimen must be prepared for transmission electron microscopy and the crystalline particulates must be properly oriented for an optimal diffraction pattern to be formed. Often, the specimen must be rotated and tilted, and diffraction patterns obtained from more than one particle orientation. Hence, for SAED studies, best results can be obtained with a transmission electron microscope which is equipped with a eucentric stage goniometer. Very thin or delicate crystalline particles may tend to degrade or disintegrate in the electron beam, interfering with formation of an interpretable diffraction pattern. In addition, theoretical considerations limit the resolution of the technique, such that with the conventional mode of SAED operation, the maximum interplanar spacing d which can be practically resolved is about 2.5 nm (most inorganic crystalline particulates, however, have d spacings smaller than this maximum value). Finally, the technique is time-consuming, so that it may not be feasible to acquire data on a large number of particles on any one sample.

X-Ray Diffraction (XRD)

The theoretical aspects of X-ray diffraction are similar to those for electron diffraction (*23*), the primary difference being that the incident radiation is an X-ray beam rather than an electron beam. Bragg's law applies to the diffraction of X-rays, and the measurement of the d spacings from the diffraction pattern permits the identification of the crystalline structure under investigation (*31*). This technique has its greatest potential in pulmonary toxicology in the identification and quantitation of inorganic crystalline particulates in the respirable range which gain access to the lung from ambient air.

The equipment for X-ray diffraction includes an X-ray source, a sample holder, and a circular camera to record the diffraction pattern on X-ray sensitive film or a detector which records the diffracted X-rays as peaks on a strip chart. The angular deviation of these X-ray maxima from the center may then be related through Bragg's law to the d spacings of the crystal structure, which may in turn be related to the d spacings of known crystalline compounds in the ASTM index. Because of the difficulty in collimating X-rays as compared to the fine beam attainable with electrons by use of magnetic lenses, X-ray diffraction is traditionally thought of as a bulk analysis technique. Thus, whereas electron diffraction can be used to obtain an interpretable diffraction pattern from a particle as small as 0.1 μm and a mass of 10^{-16} g, X-ray diffraction is performed on samples as small as 40 to 50 μm in diameter with a mass on the order of 100 ng (10^{-7} g). However, certain advanced models of X-ray diffractometers now permit examina-

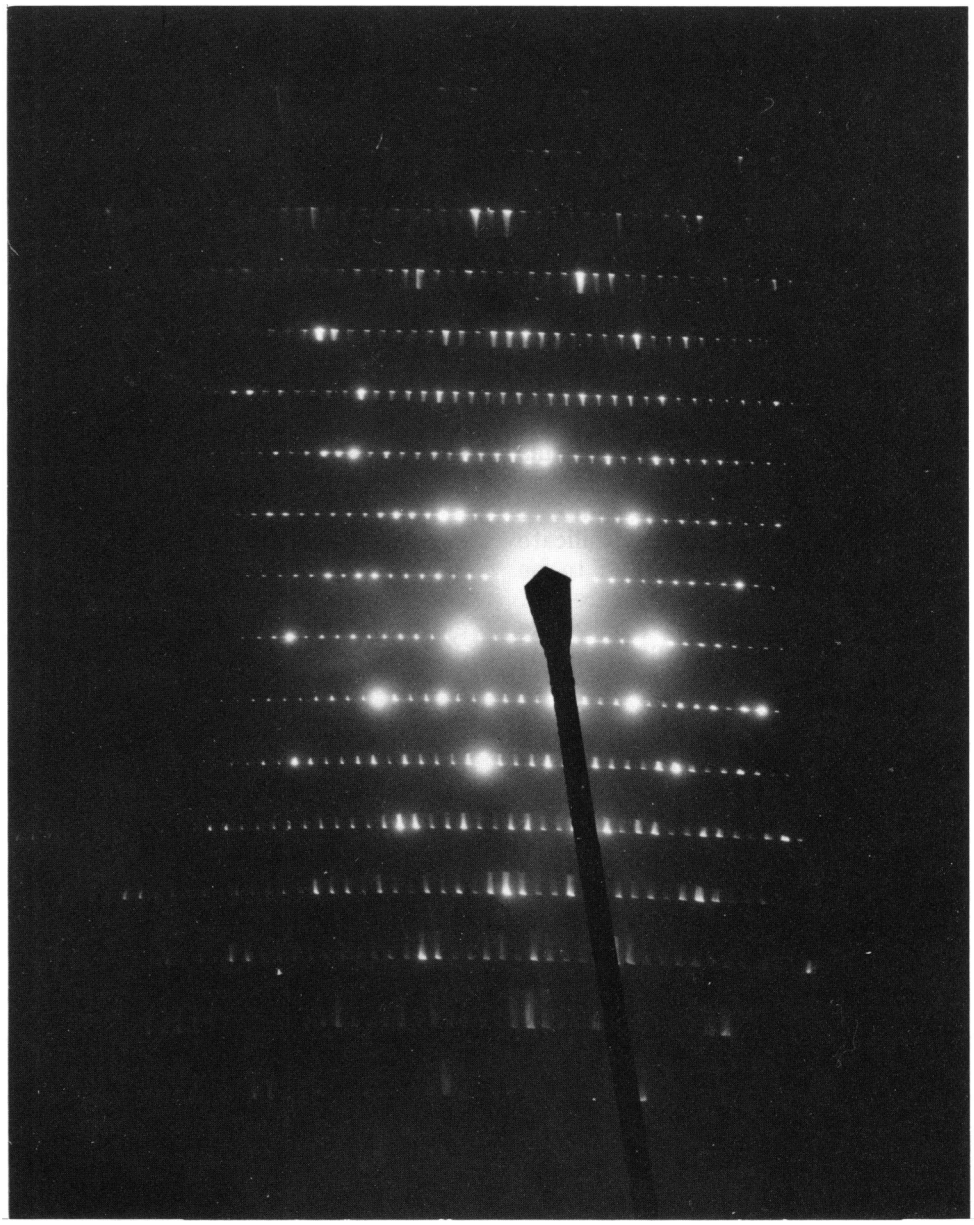

FIGURE 4. Selected area electron diffraction pattern obtained from an asbestos (ferruginous) body core of an asbestos insulation worker, with a JEM 100 C-X analytical transmission electron microscope operated at 80 kV. The pattern shows discrete dots along each layer line, with a calculated 5.3 Å interlayer-line spacing typical for amphibole asbestos.

tion of single crystals as small as 1.0 μm, with production of readily interpretable diffraction patterns (*33*). Since many bulk samples are polycrystalline (composed of large numbers of small, randomly arranged crystals) rather than a single crystal, and because the sample in an X-ray diffractometer is often rotated on the stage about the Z-axis (i.e., the axis parallel to the incident beam), the diffraction patterns obtained by X-ray diffraction as measured on film usually consist of a series of concentric rings, rather than the pattern of dots obtained from an individual submicroscopic crystal by electron diffraction. The distance from the center of the film to any particular concentric ring is inversely proportional to the d spacing between the atomic planes in the crystal which produced that ring through the diffraction of incident X-rays.

X-ray diffraction has been used in our laboratory to study the inorganic particulate content of tobacco leaf, cigarette smoke, and macrophages obtained by bronchoalveolar lavage from cigarette smokers (*34*). Because of the scattering of X-rays by the organic matrix and the resultant increase in background radiation, it is generally necessary to extract the inorganic material from

the organic matrix in order to perform X-ray diffraction studies. This may be accomplished by ashing the specimen at 500°C in a muffle furnace, suspending the residue in an appropriate spectroscopically pure solvent such as methanol/methylene chloride, and filtering onto a 0.45 μm silver filter. Alternatively, low temperature plasma ashing may be used. With either technique the filter may be rinsed with aqueous solvents to remove lung salts (e.g., NaCl). Characteristic X-ray peaks as measured on a strip chart recorder corresponding to the *d* spacings for α-quartz have been identified in tobacco leaf (seven distinct α-quartz peaks in two filtered and one unfiltered brand), cigarette smoke (up to four peaks in one unfiltered brand), and smokers' lavage macrophages (two distinct peaks in one smoker and the major 3.34 Å peak for α-quartz in another smoker) using this technique (*34*). A 10.07 Å peak has been identified in tobacco leaf, smoke, and lavage macrophage samples, which may represent the major peak for a phyllosilicate (e.g., mica). Arcanite and sylvite were noted to be present in smoke from two brands of filter cigarettes. Calcium oxalate and calcite were identified in smoke from two unfiltered brands. Finally, kaolinite which was previously identified in smokers' macrophages using energy dispersive spectroscopy and selected area electron diffraction (*25*), was identified by X-ray diffraction in lavage macrophages of one smoker (*34*). An example of an X-ray diffraction pattern and the corresponding X-ray trace are shown in Figure 5.

Although X-ray diffraction as described is generally a qualitative technique, methods have been devised by which X-ray diffraction may be used to quantitatively measure certain inorganic materials. By comparing the integrated peaks of the X-ray tracing from known standards of chrysotile asbestos with those of unknown samples and correcting for X-ray absorption by the matrix and the filter, investigators have demonstrated that it is possible to measure chrysotile in microgram quantities with good precision, and with detection limits as low as 3 $\mu g/cm^2$ of filter when chrysotile is present in small quantities (1% by weight of matrix material) (*32*). Quantitative X-ray diffraction has also been used to measure the amount of α-quartz present in lung tissue, with a sensitivity of as little as 50 μg of quartz in 1 mg of inorganic ashed residue (*30*). Such techniques hold great potential for the identification and measurement of these and other inorganic particulates present in lung tissues.

Selected area electron diffraction has the advantage of its ability to analyze the crystalline structure of individual submicron particles in a sample, even in the presence of an organic matrix provided the sample is thin enough to permit transmission of electrons. However, the method is time-consuming, and particle selection bias could occur because of the limited number of particles which can reasonably be analyzed per sample. X-ray diffraction, on the other hand, is primarily a "bulk" technique, and can readily give information on the crystalline structures present in an unknown sample. Disadvantages include the requirement that the material to be analyzed be extracted from its organic matrix, with resultant possible loss or modification of the inorganic materials of interest. Also, in quantitative X-ray diffraction analysis, variations in particle size distribution between samples containing the same quantity of crystalline material can result in changes in the X-ray line intensities (*30*), and interference from other related mineral species present in the sample can lead to inaccuracies in quantitative determinations (*32*).

X-Ray Analytical Techniques

X-Ray Fluorescence (XRF)

The technique of X-ray fluorescence (XRF) involves measuring the characteristic energy (or wavelength) of X-rays emitted from atoms in a sample when higher energy level electrons drop down to fill vacancies left by ejected lower energy level electrons. The technique differs from electron microscopy/energy dispersive X-ray analysis (EDXA) in that the incident radiation which provides the energy for displacing the low energy level electrons is an X-ray beam in XRF, whereas it is a finely focused electron beam in EDXA. Because of the difficulties in collimating an X-ray beam referred to in the previous section, XRF is essentially a macro or bulk analytical technique, and generally cannot be used to determine the chemical composition of an individual microscopic particle.

The instrumentation for XRF consists of an X-ray source (e.g., a transmission target X-ray tube), a specimen holder, an X-ray detector (e.g., a lithium-doped silicon crystal and energy dispersive spectrometer or a wavelength dispersive crystal spectrometer), and a pulse analyzer or pulse processor-computer interface. The X-ray beam diameter typically ranges from 0.1 to 1.0 cm with a minimum analytical volume of 8×10^{-6} cm^3 (*7*). The minimum detection limit is 2×10^{13} atoms with a relative detection limit in the range of 1 to 100 ppm. This degree of sensitivity is on the order of two orders of magnitude greater than that for the electron microscopic techniques discussed above. A scanning electron microscope equipped with an energy dispersive spectrometer can be readily modified for use as an XRF device (*35*). This can be accomplished by placing a thin metal foil in the electron beam, which generates characteristic X-rays whose energies depend on the elemental composition of the foil. These X-rays are transmitted to the specimen which then emits characteristic X-rays depending on the elemental composition of the specimen and the energy of the exciting X-rays. The material composing the target foil is so chosen that the energy of the characteristic X-rays produced exceeds the X-ray absorption edges of the elements of interest in the specimen. In addition, the foil and its housing are designed so that the incident

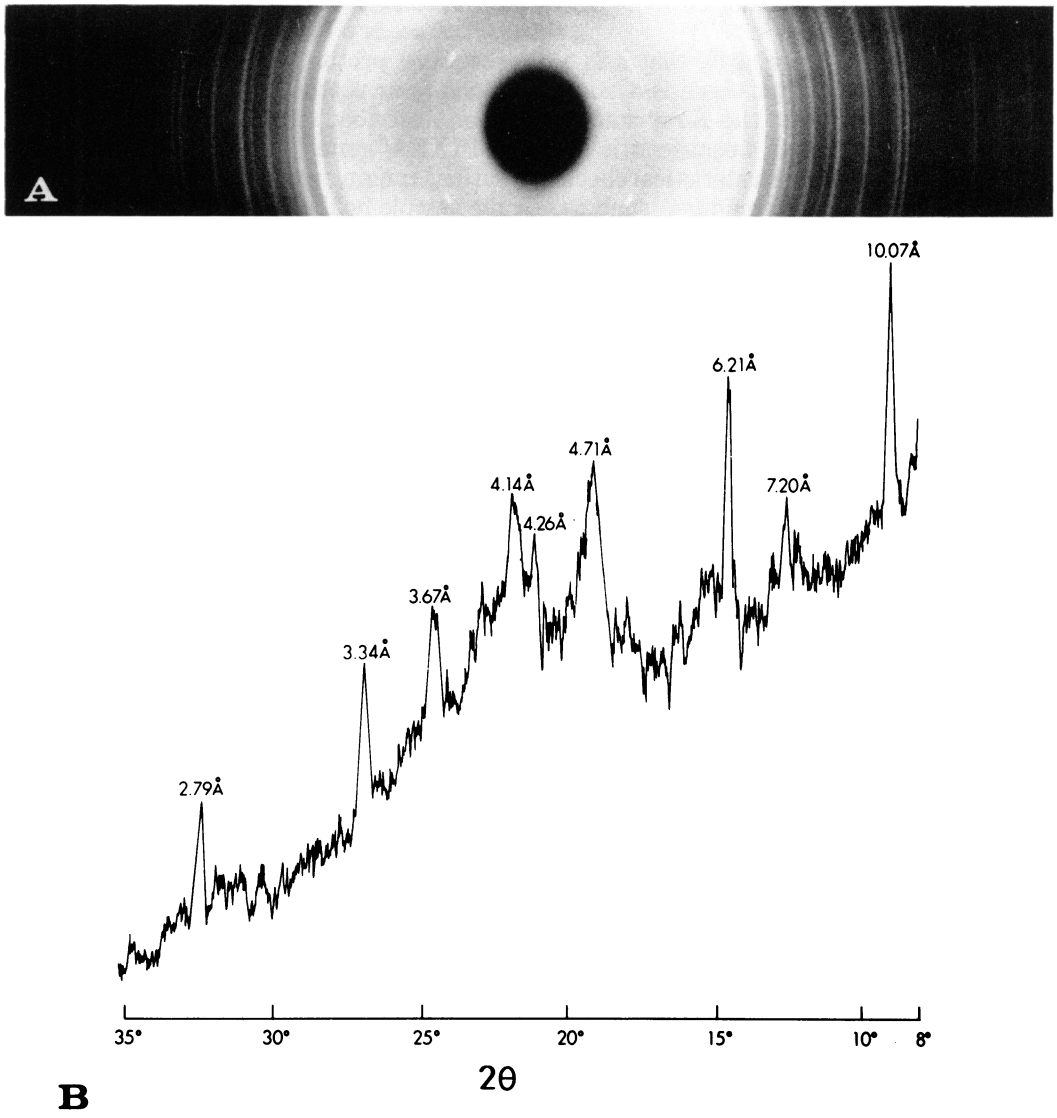

FIGURE 5. X-ray diffraction pattern (*A*) and tracing (*B*) obtained from an unfiltered brand of cigarette smoke (see text). The tracing shows peaks corresponding to the 3.34 Å and 4.26 Å lines for α-quartz, the 6.21 and 3.67 Å peaks for calcium oxalate, and the 7.20 Å peak for kaolinite. The 10.7 Å peak may represent mica (a phyllosilicate). Numerous additional lines are visible on the X-ray film.

electrons are totally absorbed or shielded from the specimen, most of the Bremsstrahlung (continuum background) radiation is absorbed by the foil, and most of the X-rays generated in the foil are transmitted to the specimen while being shielded from the X-ray detector. A 0.025 mm molybdenum foil excited by an incident 30 kV electron beam meets most of these requirements and is sensitive to elements whose X-ray spectra extend up to the 17 keV range (*35*). When the analytical SEM is modified in this way, the investigator is sacrificing spatial resolution to obtain increased elemental sensitivity; in some circumstances, this set of conditions offers certain practical advantages.

X-ray fluorescence has been used in the scanning electron microscope (XRF/SEM) to qualitatively measure the elemental composition of coal fly ash, with identification of trace elements not resolvable by conventional EM/EDXA, and with a much improved peak to background ratio of from 10- to 50-fold (*35*). This technique may be used to rapidly and accurately analyze the chemical composition of particulate material collected on a filter from air or water samples. XRF/SEM may be used in conjunction with EM/EDXA, rapidly providing data that may be used as a statistical check on analyses of elemental composition based on a population of particles examined individually (particle by particle) with EM/EDXA. In this way, XRF/SEM may indicate whether the particles sampled by EM/EDXA are in fact representative of the entire population of particles in the specimen. XRF/SEM might also be a useful technique for measuring nonparticulate trace elements (such as lead, cadmium, nickel or

chromium) in sections of lung tissue or alveolar macrophage pellets.

The disadvantages of XRF are primarily that it is a bulk or averaging technique, and that there is a wide variation in sensitivity, depending on the X-ray source and detector (*7*). On the other hand, because it is an averaging technique, it can be used as a statistical check on selection bias of microanalytic techniques, such as EM/EDXA. Advantages of XRF include its increased sensitivity over a wide elemental range as compared to EM/EDXA, increased peak to background ratio, and decreased associated Bremsstrahlung (background) radiation. X-ray-induced X-ray emission gives rise to another type of background, however, called Compton scattering, which ultimately determines detection limits. In addition, it has an increased depth of specimen penetration as compared to some other analytical techniques, such as AES, SAM, and SIMS (discussed below); it does not destroy the specimen; and it is not subject to interferences related to charging of the sample.

Proton-Induced X-Ray Emission Analysis (PIXEA)

In previous sections, the emission of characteristic X-ray photons by a sample bombarded by X-rays (x-ray fluorescence) or by an electron beam (EDXA) was discussed. X-rays may similarly be generated from a sample by bombardment with a proton beam, and the X-rays possess energy (or wavelength) properties indicative of the elemental composition of the bombarded portion of the sample. This technique, called proton-induced X-ray emission analysis (PIXEA), has promising potential for trace analysis. The instrumentation consists of a Van de Graaf accelerator which serves as a proton source, a beam diffuser and carbon collimator for obtaining a focused proton beam, sample holder, vacuum chamber (5×10^{-5} Torr), and an X-ray detector and analyzer. Beam energies are typically in the range of 2.5 to 3.0 MeV, with a proton beam diameter of 0.2 to 2.0 cm and beam current of 2 to 150 namp. The spectral resolution of the 30 mm^2 Si(Li) detector is typically 145 eV at the 5.89 KeV Mn Kα line. The precision of the technique is within ± 2%, and PIXEA is sensitive for many elements in the less than ppm range (values for optimum sensitivity for several elements of interest in pulmonary toxicology are given in Table 2) (*37*). A scanning proton microprobe instrument employing a much finer proton beam (approximate 10 μm) has also been described (*3,36*).

PIXEA generally requires minimal sample preparation, ranging from directly mounting the specimen in the sample holder to placing a tissue section on a plastic sheet stretched over a graphite ring, or mounting a filter from an environmental sample onto the holder with a small amount of adhesive material. Lyophilized tissue may also be compressed into a pellet, providing a convenient sample for PIXEA. This technique has been used to analyze the trace element content of pigmented versus nonpigmented areas in sections of freeze-dried, formalin-fume inflated lung. Direct analysis of 5–mm thick sections of these lung preparations was not possible because the porosity of the specimen led to wide fluctuations in the Bremsstrahlung background level. Samples of pigmented and nonpigmented lung tissue were therefore prepared by ashing with concentrated HNO_3 and H_2SO_4 (2:1), followed by evaporation to dryness, redissolving in dilute HNO_3 and deposition on a Nuclepore filter. PIXE analyses indicated that for those samples with relatively high levels of Zn and Pb, there is a disproportionate concentration in the pigmented areas (*60*). Other investigators have used PIXEA to demonstrate a nonhomogeneous distribution of titanium, chromium, nickel, and strontium within lung tissues, suggesting that the source of these trace elements is atmospheric pollution (*61*). Further studies are required on more lung tissue samples and for other trace elements, so that these data may be correlated with smoking history, occupation, and pathological findings. PIXEA may also be of value in toxicologic studies of trace metal poisoning in tissues of man or experimental animals and has been used to study the elemental content of filters prepared from various air and water samples (*60*). An example of a PIXEA spectrum is shown in Figure 6.

The advantages of PIXEA include its high sensitivity in terms of absolute and relative elemental abundances, simultaneous multielemental analysis, nondestructive nature, ease of sample preparation, and rapidity of data acquisition (typically 1 to 15 min per sample). In addition, it has the potential for near-surface analyses,

Table 2. Approximate sensitivity of several analytical chemical techniques for selected elements of interest in pulmonary toxicology.[a]

Element	Detection limits, ppma			
	Atomic absorption	ICP-AES	PIXEA	Neutron activation
Al	0.006–0.1	0.02	~1000	0.004
Cd	0.0002–0.0004	0.001	2	0.005
Cr	0.002–0.006	0.004	5	0.3
Ni	0.008–0.01	0.006	2	0.7
Pb	0.002–0.013	0.020	3	0.5
Si	0.03–0.2	0.010	~1000	3[b]
Zn	0.0001–0.0002	0.001	1	0.1

[a] Data from the literature (*45,54–59*)
[b] Detection limit in μg/sample.

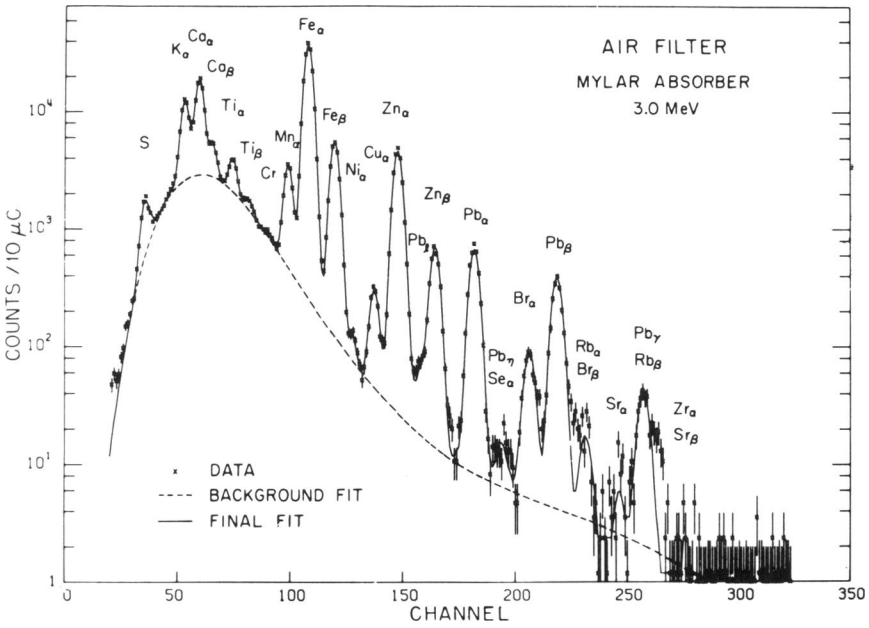

FIGURE 6. PIXE spectrum obtained from an urban air sample collected on a Nuclepore filter. Channel number (abscissa) is proportional to the KeV of the X-rays detected. Note the logarithmic scale on the ordinate. The prominent peaks for iron, titanium, and lead are commonly identified in urban air samples with this technique.

since the effective proton penetration can be limited to less than a 50 μm depth. Disadvantages include the requirement for access to a proton accelerator, and problems in dealing with liquid samples (e.g., these must be dried or filtered, and volatile components may be lost due to placement in a vacuum or mild heating by the proton beam). In addition, sensitivity limits are affected by interelement interferences and by matrix effects (especially for light elements) (*37*), and the sensitivity for aluminum and silicon is poor (Table 2).

Microprobe Mass Spectrometry

Secondary Ion Mass Spectrometry (SIMS)

This technique involves the interaction of an energetic primary ion beam with a solid specimen (*62–65*). A primary ion is either backscattered from the surface layer (a low probability event at KeV primary ion energies typical for SIMS), or it enters the solid and dissipates energy via collisional cascades with lattice atoms. Removal of surface material (ion sputtering) occurs when some of the recoiling atoms within a few atomic layers of the sample surface acquire sufficient kinetic energy to escape from the solid. A small fraction of the sputtered species are ions, and thus are directly available for characterization using mass spectrometry. The sputtering process permits depth-profiling of the elemental composition of the sample. The depth resolution of the technique is excellent since secondary ion escape depths are on the order of a few atomic layers. Subsurface mixing of the sample constituents primarily due to sputter induced collision cascades limits the experimental depth resolution to about 10% of the depth sputtered, e.g., 100 Å at a depth of 0.1 μm into the sample.

The elemental detection sensitivity for SIMS is dependent upon a number of experimental factors including the primary ion composition, energy, and current density; the sample matrix composition and its sputtering rate; and instrumental parameters relating to energy and mass discrimination of the secondary ions (*17*). For a given set of primary ion and spectrometer conditions, elemental sensitivity may vary by as much as six orders of magnitude owing to variations in ionization efficiency and sputter/ion yields with atomic number. Control of primary ion composition and the detection of both positive and negative secondary ions can be used to enhance SIMS sensitivity for a given element. In the absence of mass spectral interferences requiring high mass resolution and with optimization of primary ion beam characteristics, most elements are detectable at the ppm level. For example (*17*), electronegative oxygen in a variety of ionic states can be used as the primary ion (O_2^+,O^-) to enhance the positive secondary ion emission for elements having low ionization potentials. Electro-positive cesium can be used as the primary ion (Cs^+) to enhance the negative secondary ion emission for elements with high electron affinities. Many elements of physiologic importance (e.g., Na, K, Mg, Ca, S, Cl) or toxicologic interest (e.g., Li, Be, Si, Ti, V, Cr, Mn, Se, As, Pb) may be detected at concentrations substantially lower than those available

with many conventional techniques including EDXA. The enhanced sensitivity of SIMS may be exceedingly important for controlled *in vitro* or *in vivo* inhalation studies involving low dose exposures or ambient air samples that may contain potentially toxic species at only trace concentrations (*8*).

For studies requiring a high degree of lateral spatial resolution, SIMS must be employed in a microanalytical mode. There are two basic SIMS instrumental configurations, the ion microanalyzer and the ion microprobe, that achieve lateral resolutions on the order of 1 μm for biological specimens (*15*). The ion microanalyzer utilizes secondary ion optics to obtain a final mass resolved ion image having a one-to-one correspondence with the lateral concentration distribution of the element on the sample surface. The primary ion beam diameter (typically on the order of 50 μm) does not limit the lateral resolution available with the ion microanalyzer. The ion microprobe uses focused primary ion beams having diameters as small as 1 μm. Smaller beam diameters and corresponding lateral resolutions currently are limited by sensitivity considerations, but beam diameters below 0.1 μm are expected in the near future. The secondary ion emission from the sample surface modulates the intensity of an oscilloscope whose $x-y$ deflection is synchronized with the ion microprobe primary beam raster scan (analogous to SAM or SEM/EDXA elemental dot mapping). Both the ion microprobe and microscope are capable of three-dimensional characterization since repetitive images will be acquired at progressively larger depths into the sample. This analysis mode will benefit greatly from rapidly evolving techniques involving computer-assisted digital image processing (*66*).

Previous SIMS studies have shown that many types of air pollution particulates preferentially concentrate toxic chemicals on their surfaces where they are most directly available to biological fluids or cells following inhalation or ingestion (*8*). The interfacial chemistry governing the migration of toxic species from particle surfaces into lung fluids or cells (e.g. alveolar macrophages) is, therefore, of considerable interest. We are using SIMS to study the uptake, localization and chemistry of toxic particles *in vitro* within rabbit alveolar macrophages (RAMS) in tissue culture and monolayers. Frozen RAM sections are analyzed with 10 to 12 KeV O_2^+ primary ions using a Cameca IMS-3f ion microscope (*16*). A specimen section thickness between 0.25 and 0.5 μm is optimal, since it has a sputter lifetime sufficient for multielemental SIMS analyses, and yet is thin enough to avoid electrical charging artifacts and to permit pre- and post-SIMS TEM characterization of cell ultrastructure when sections are mounted on TEM grids.

An example of the elemental sensitivity available using ion microanalysis is shown in Figure 7 for whole RAM control cells dispersed on an aluminum foil substrate. Individual RAMs about 15 μm in diameter are visible as dark areas in the $^{27}Al^+$ secondary ion image. The corresponding $^{39}K^+$ image shows excellent localization to the individual RAM cells and was acquired using an exposure time of only 0.02 sec. Similar sensitivities were observed for other physiologic elements including Na, Mg, Ca, all of which required much less than 1 sec to acquire individual secondary ion images thereby optimizing depth resolution. A recent study of the uptake of 5 μm Pb_3O_4 particles in RAMs (*16*) demonstrated that SIMS can be used as a depth profiling tool to monitor the penetration of toxic lead-containing species into the interior of macrophage cells. Furthermore, secondary ion images suggested that Pb was associated with the formation of Pb precipitates containing P and Ca in the cytoplasm. Ion microanalysis also has been used to study Be in lung tissues of individuals having berylliosis (*14,49*) and to study the distribution of aluminosilicate particles in macrophages present in bronchoalveolar lavage fluid obtained from a cigarette smoker. With regard to the latter, the localization and association of Al and Si with secondary ion imaging is shown in Figure 8, and is consistent with previous results using SEM/EDXA (*52*). The $^{56}Fe^+$ map highlights cell outlines, since both iron particles in lysosomes and ferritin molecules distributed diffusely throughout the cytosol contribute to the image. The circular iron-depleted areas correspond to individual macrophage nuclei.

In summary, the advantages of SIMS include potentially high elemental sensitivity, broad elemental coverage, isotopic sensitivity, and three dimensional chemical analysis. The limitations of SIMS include the inherently destructive nature of the technique and nonidealities of the sputtering process leading to preferential or selective sputtering of individual components present in heterogeneous solids. In biological specimens, this may lead to selective removal or retention of organelles, membranes, or other subcellular components. Figure 9 shows the results of TEM studies of macrophages before and after exposure to a 10 KeV O_2^+ primary ion beam used to obtain the secondary ion images in Figure 8. It is apparent that certain organelles (e.g., nuclei, lysosomes), may sputter faster than the surrounding cytoplasm. Hence, secondary ion images may show variations that are in part sputter yield dependent, rather than being dependent solely upon actual lateral concentration variations.

Laser Microprobe Mass Analyzer (LAMMA)

Another technique involving mass spectroscopic analysis of ions emitted from a sample is the laser microprobe. A finely focused laser beam is directed onto the sample surface, and a short pulse from the laser is used to vaporize and ionize a portion of the sample. The commercial instrument (LAMMA) consists of a light microscope (with phase optical and darkfield capabilities) for focusing the laser on the sample surface, a laser source, a sample holder, secondary optics and

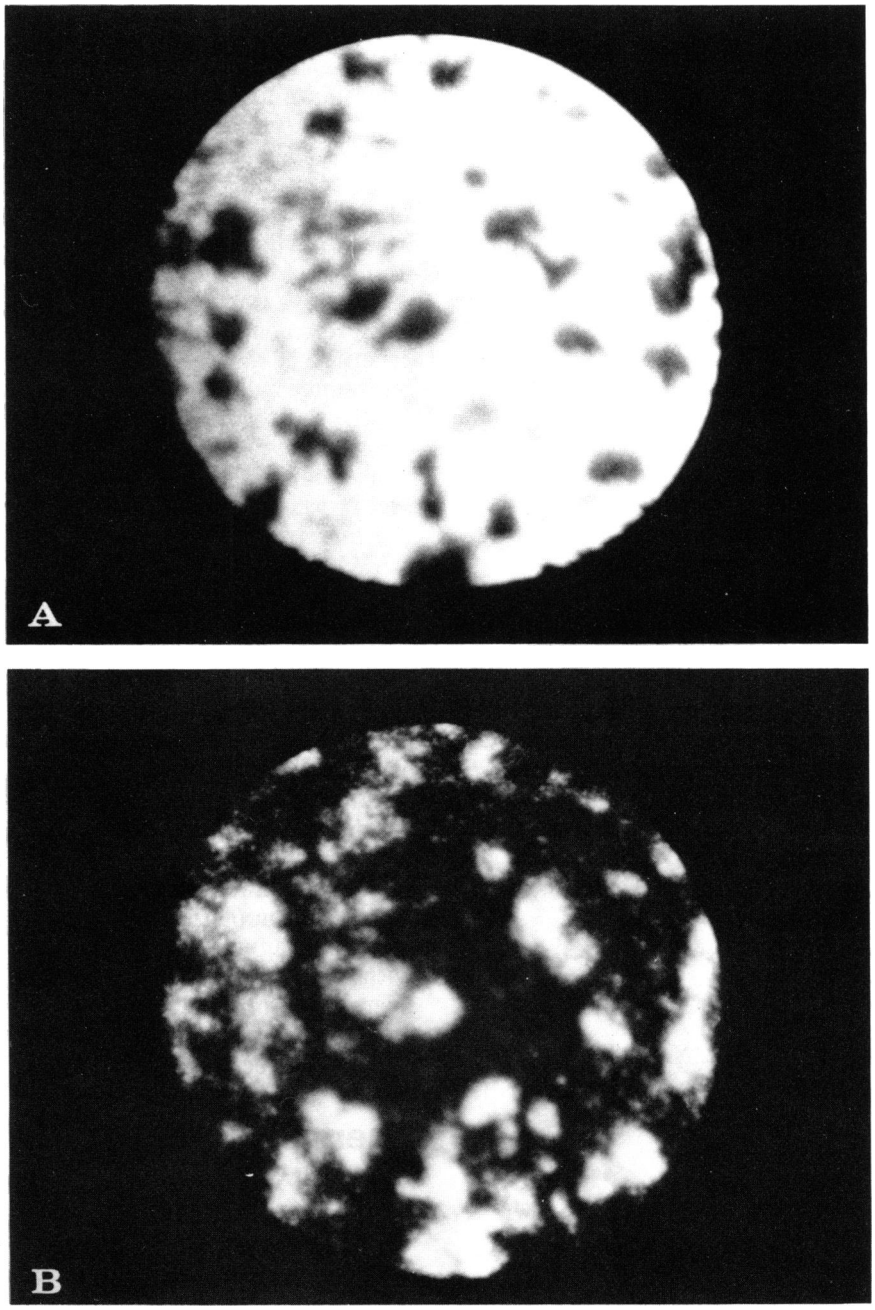

FIGURE 7. Secondary ion micrographs of rabbit alveolar macrophages on an aluminum substrate, magnified × 500: (*A*) aluminum image ($^{27}Al_2^+$), exposure time 1/15 sec; (*B*) potassium image ($^{39}K^+$), exposure time 1/60 sec. From Linton et al. (*16*), with permission.

mass analyzer. The LAMMA employs a time-of-flight mass spectrometer (*22*) for rapid data acquisition which is essential because of the pulsed (nanosecond pulse widths) nature of the ion source. The laser beam diameter is approximately 2 μm, with a lateral spatial resolution as small as 0.5 μm. The relative detection limit for many elements is in the range of a few tenths to 20 ppm atomic, with an absolute detection limit of 2×10^3 atoms and a minimum analyzed volume of $10^{-13}cm^3$ (*22*). The best reproducibility from one pulsed analysis to the next is ± 5%, and the mass spectrum obtained with each pulsed laser analysis can be stored in a fast transient digital recorder for further data processing (*18*).

The LAMMA was designed primarily for the analysis of the composition of thin films, with an optimal sample thickness in the range of 0.1 to 2.0 μm. For soft biological specimens, sample preparation generally involves shock-freezing, freeze-drying, sectioning and plastic embedding under a vacuum. Particulate material

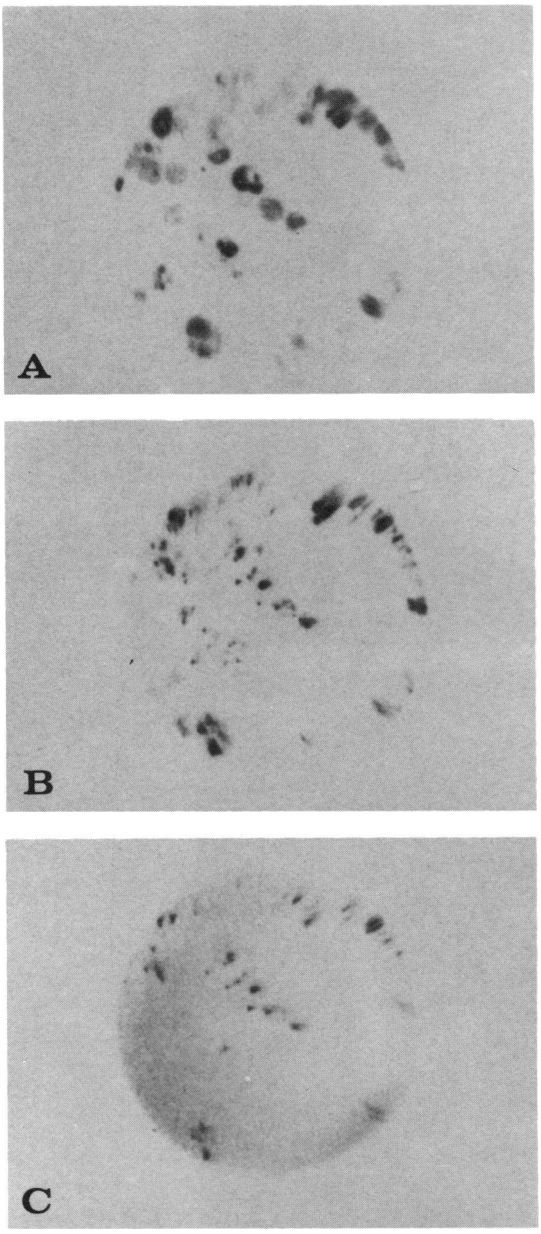

FIGURE 8. Secondary ion micrographs of human alveolar macrophages obtained by lung lavage from a heavy cigarette smoker (same specimen as Fig. 9). The cells were fixed with glutaraldehyde only and embedded in epoxy resin. Maps are illustrated for the distribution of (*A*) iron, (*B*) aluminum and (*C*) silicon. Magnified ×267; reverse contrast images (darker areas represent higher elemental concentrations).

should be evenly distributed on a conventional electron microscopic grid coated with a chemically clean support film such as formvar, mylar, or carbon. The Laser microprobe mass analyzer (LAMMA) has been used to study urban aerosol particulates, asbestos fibers, and coal mine dust, and is capable of analyzing particles as small as 0.1 μm diameter (*19,20*). Quantitative results can be enhanced if the volume of a completely vaporized (no residue or recondensate visible) particle, ion yield of the elements present, and the ion/electron conversion efficiency of the secondary electron multiplier of the mass analyzer are all known (*18*). Studies of asbestos fibers have shown that the mass spectra obtained allow easy discrimination among crocidolite, amosite, and chrysotile fibers, as well as detection of a number of trace contaminants. In addition, LAMMA may be used to detect the presence of trace toxic elements, such as cadmium, lead, and strontium, in biological materials (*18*).

The advantages of LAMMA include its sensitivity for many elements in the ppm atomic range, with broad coverage of the periodic table. Individual particles can be sequentially and very rapidly analyzed, and like SIMS, the technique has the potential for isotopic and organic chemical analyses (*21*). The ion yield is dependent primarily upon ionization potential of an element and appears less dependent on the chemical nature of the matrix in comparison to SIMS. The sensitivity of LAMMA for singly charged ions with ionization energy of 4 to 8 eV varies over an order of magnitude, whereas the sensitivity of SIMS may vary over three orders of magnitude. The LAMMA also may be more sensitive than SIMS in the analysis of some heavy metals such as lead (*18*). The disadvantages of LAMMA include the limitation of light microscopic resolution, measurement of either positive or negative ions (but not both) in vaporization of a single particle, limitation to analysis of specimens with a thickness in the range of 0.1 to 2.0 μm, and destruction of the sample during the analytical process. The mass resolution of the time of flight mass spectrometer of the LAMMA instrument is about an order of magnitude less than that potentially available with the double-focusing mass spectrometers of the ion microprobe or microanalyzer (SIMS). This may be of particular concern in the analysis of chemically complex biological specimens.

Chemical Techniques

Atomic Absorption Spectrometry (AAS)

Atoms of a given element in an unexcited or ground state will absorb radiant energy at specific wavelengths, characteristic of the element. When these atoms are placed in a beam of radiant aenergy of these specific wavelengths, they will absorb an amount of the radiant energy which is proportional to the number of atoms present, or if the sample volume is fixed, to their concentration. This is the principle of atomic absorption spectrometry, a technique which is used to measure trace metals in solution samples in the part per million to part per billion mass range (*54,55,57*). The atoms in the sample may also emit radiant energy at the same wavelength which is absorbed, a factor which must be considered when measuring the absorbed light in quantitative determinations (*39*).

The source of the radiant energy of specific wave-

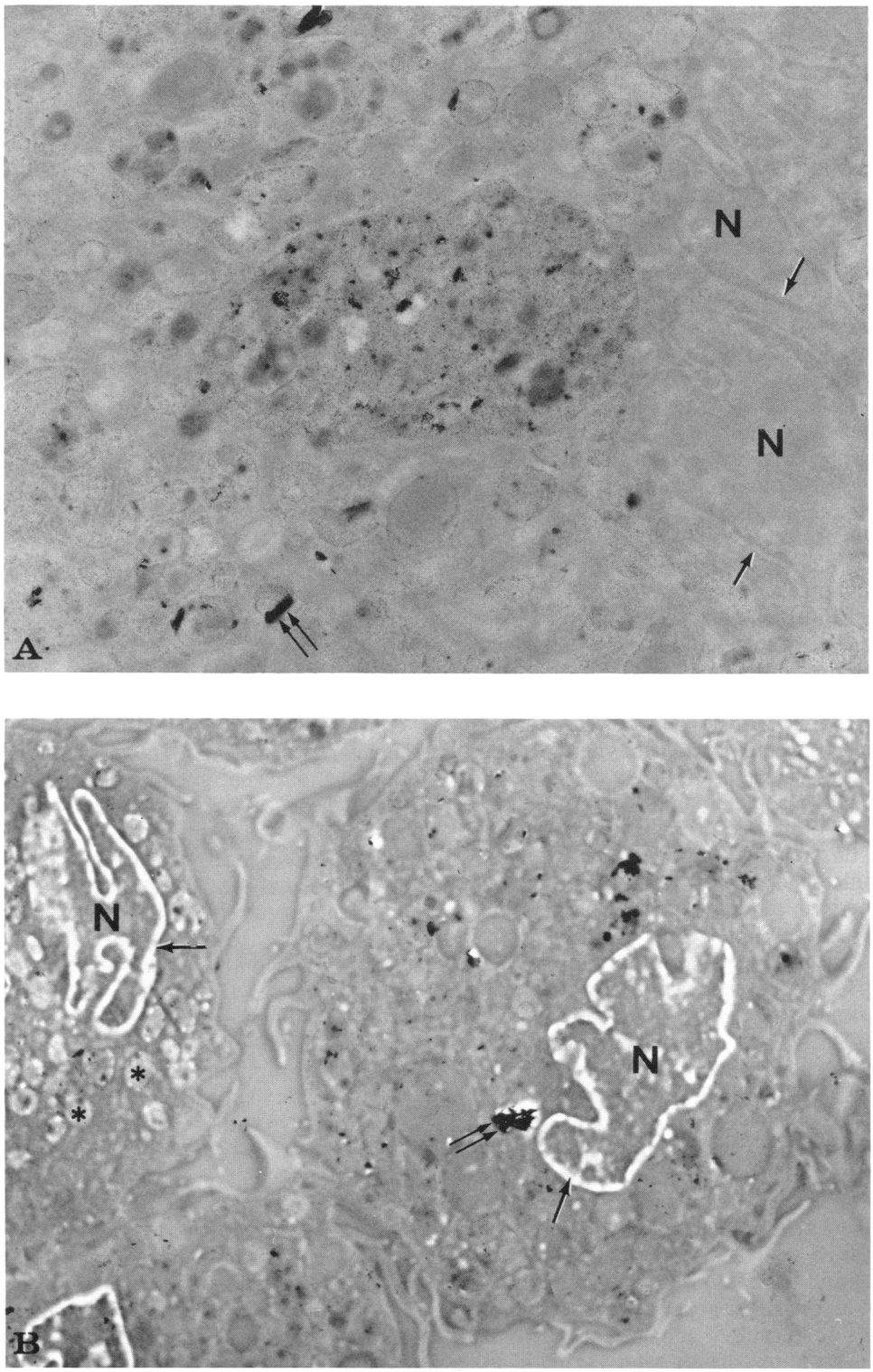

FIGURE 9. Conventional thin section of a human alveolar macrophage from a heavy cigarette smoker (same specimen as Fig. 8) is shown in *A*. The cells were fixed with glutaraldehyde only; consequently, only inherent tissue and foreign particle contrast is seen. A portion of a single alveolar macrophage shows numerous particles of aluminum silicates and other xenobiotics in lysosomes (double arrows), and two lobes of the nucleus (N) are discerned. The nuclear envelope (single arrows) and associated heterochromatin are intact. The same field is illustrated in *B* after considerable sputtering from the secondary ion beam. There is marked loss of heterochromatin associated with the nuclear envelope (arrows). Nuclei (N) therefore stand out in bold relief. A suggestion of preferential lysosomal etching is also seen (asterisks). Some particles (double arrows) appear relatively resistant to etching. Transmission electron microscopy. Magnification: (*A*) ×12,500; (*B*) ×6,300.

length is either a hollow cathode lamp or an electrodeless discharge lamp. The sample is introduced into the radiant energy beam in a flame by aspirating sample solution into the flame, wherein the solvent evaporates leaving minute crystals of sample, which are subsequently vaporized and atomized. The particular wavelength to be measured is selected with a suitable monochromator and measured with a detector with amplifier and readout system. Modulation of the radiant energy power supply to the hollow cathode is frequently used, so that the emitted light from the atoms of the sample itself (which is steady) can be electronically subtracted and only the light absorbed by the sample is actually measured. As many as 67 elements can be detected by atomic absorption spectrometry, and the relative detection limits for many elements are in the range of 0.0003 to 0.2 ppm atomic. When a double-beam or dual-channel procedure is employed to compare the intensity of the incident and transmitted light, the precision of the technique is better than ± 1% (*40*). A comparison of sensitivities among atomic absorption spectrometry and other chemical techniques (to be discussed subsequently) for some elements of interest in pulmonary toxicology is shown in Table 2.

Analysis of trace elements in lung tissues or alveolar macrophages by conventional atomic absorption requires a digestion-extraction technique, since the sample must be in solution. One approach is low temperature plasma ashing (under a nascent oxygen stream) of the specimen with dissolution and/or suspension of the residue in a spectroscopically pure solvent. Some elements, such as aluminum and silicon, when encountered in lung tissue, are in forms which are difficult to solubilize; this difficulty may be circumvented by fusion with highly purified molten borate salts and dissolution of the resultant mixture in weak acid solution. A modification of the atomic absorption spectrometer described above permits analysis of microsamples (10–50 μL) with enhanced sensitivity (ppb atomic). The technique, known as electrothermal vaporization (atomization) atomic absorption involves flameless atomization of the sample. This is accomplished by placing the sample solution in a carbon tube which is heated electrically to vaporize the sample; the incident radiant energy passes through the vaporized sample in the carbon tube and the absorption at a given wavelength is measured (*41*). We have used atomic absorption spectrometry to measure the levels of trace elements in ashed lung tissue, and have found that nickel, zinc, and to a lesser degree lead, are present in higher concentrations in the lungs of cigarette smokers than in nonsmokers. Nickel is a known trace component of cigarette smoke (*67,68*).

As a bulk technique, atomic absorption is an excellent method to measure the trace metal content extracted from lung tissues, because of its high sensitivity, accuracy and precision, simplicity, and relative inexpensiveness. Disadvantages of atomic absorption include spectral and chemical interferences, although the former can often be circumvented by selecting a wavelength in the absorption band which is free of interferences from the particular sample under evaluation (although this may be at the expense of some sensitivity). Chemical interferences include formation of stable oxides, which reduce the number of free atoms in the unexcited state and hence reduce the sensitivity, and interference from some anions (such as interferences from phosphate in the measurement of calcium) (*39*). Problems related to continuous and band emission from the flame and the methods of eliminating these interferences were described in previous paragraphs. One final disadvantage of the technique is that it is severely limited with respect to simultaneous multielemental analysis (*69*).

Inductively Coupled Plasma-Atomic Emission Spectroscopy (ICP-AES)

As noted in the discussion of atomic absorption, elements will emit as well as absorb light at very specific wavelengths corresponding to quantitized electronic transitions. The intensity of the emission will be proportional to the concentration of the given element in the sample. This phenomenon is the basis of atomic emission spectroscopy, which is used for simultaneous measurement of many elements in the part-per-million mass range. The recent development of a very efficient energy source for vaporization-atomization-excitation-ionization of a sample at high temperatures (5500–8000°K) has greatly increased the utility of this method for trace analysis. The energy source is the inductively coupled, argon plasma. Argon is passed through a quartz tube, which is surrounded by a metal coil through which alternating current at a frequency of 20 MHz is passed. A spark is introduced into the argon, which produces a few free electrons and argon cations. The oscillating electrical field produced by the current flowing through the coil causes these ions to collide with argon atoms to produce more ions and intense heat. The inductively coupled argon plasma results in virtually complete atomization of nebulized samples introduced into the plasma (*42*), and it has broader elemental coverage than atomic absorption spectroscopy.

The instrumentation for inductively coupled plasma-atomic emission spectroscopy (ICP-AES) includes an inductively coupled plasma-nebulizer module, a radiofrequency (approximately 30 MHz) generator as an energy source for the plasma cell, a spectrometer, and a readout system. The spectrometer may either be a polychromator consisting of a diffraction grating with precisely located exit slits, each with its own photomultiplier tube, to isolate the spectral lines of interest, or a scanning monochromator with computer interface for sequential analysis of the spectral lines of interest. The polychromator plasma system is capable of simultaneously detecting up to 48 elements at the rate of up to

600 analyses per hour. Scanning monochromator systems are less efficient, but permit the measurement of a number of lines per element to enhance the reliability of the analysis. Echelle monochromators coupled to photodiode array detectors will enhance the capabilities of ICP-AES with respect to simultaneous multielement analysis. Linearity of the technique for many elements extends over a range of five orders of magnitude, with a precision of ± 1% or better.

ICP-AES is a bulk chemical analytic technique, and preparation of biological tissues or inorganic powders for analysis involves dissolution (or fusion for inorganic powders), suspension in an aqueous solution, nebulization, and injection into the ICP stream. Tissues may be lyophilized and homogenized, ashed in a muffle furnace at 550°C, and the residue extracted in 2% HNO_3 (*43*). Materials with a high silicate content are difficult to measure by ICP-AES because of inherent insolubility. An acceptable procedure has been described which involves dissolution with hydrofluoric acid in a Teflon bomb. Analyses of coal fly ash using this technique provided data quite comparable to the National Bureau of Standards analysis of the same sample. The disadvantage of the Teflon bomb is its impracticality for multiple sample analyses (*44*). Despite the sensitivity of ICP-AES over a wide range of elemental concentrations, there is a paucity of published data relevant to pulmonary toxicology.

The advantages of ICP-AES include its elemental sensitivity and linearity of response over a wide concentration range. The technique is simple with minimal chemical interferences. There is a high degree of precision with rapid simultaneous or sequential data acquisition for a large number of elements. Disadvantages of the technique include requirement for extraction of biological or particulate samples to obtain a solution which can be nebulized for atomization (as is true for atomic absorption analysis). Extracts of biological samples may cause plugging and obstruction of the nebulizer. Monitoring of the alignment system of polychromators is required to detect misalignment and drift, which can affect the analytical results. Background shifts and stray light may also introduce analytical bias and should be corrected. Also, nonidealities of the aerosol-generation processes may limit the precision which is attainable by ICP-AES (*42*). A final limitation of the technique arises from the high energy of the plasma source, with resultant ionization of many of the atoms in the sample and emission of wavelengths of radiant energy distinct from those emitted by the nonionized atoms of the sample. Overlap of the wavelengths from the ionized atoms with the wavelengths of interest (i.e., nonionized atoms) may potentially result in poor resolution, so that the wavelengths to be detected and measured for any particular element must be carefully selected. On the other hand, the high ion populations are now being exploited with the development of the ICP as an ion source for inorganic mass spectrometry.

Neutron Activation Analysis (NAA)

This trace element technique requires the bombardment of the sample by neutrons from a nuclear reactor, and subsequent measurement of the radioactive isotopes produced using high resolution gamma-ray spectrometry wherein emitted gamma rays are characteristic of the elements present. The instrumentation required includes an atomic reactor to provide a neutron source, a lithium drifted germanium gamma-ray spectrometer, and a multichannel pulse height analyzer. Standard samples of known concentration are prepared to obtain calibration curves. Under optimal conditions, the precision of the technique is better than ± 1% (*45*).

Neutron activation has been utilized to measure levels of trace elements in a number of human tissues obtained at autopsy (*46,47*). Samples were prepared by wrapping freeze-dried tissue in a polyethylene film followed by long-term irradiation for 18 hr or by grinding freeze-dried tissue to a fine powder, wrapping in a polyethylene film, and placing in a reactor for short-term irradiation (3 min). For short-term irradiation, the thermal neutron flux ranged from 1 to 1.5 × 10^{12} neutrons/cm^2/sec, and the samples and standards were counted for 3 min. For long-term irradiation, the thermal neutron flux was 5 × 10^{11} neutrons/cm^2/sec, the standards were counted for 100 to 300 sec, and the samples were counted for 3000 to 5000 sec. Energy resolution of the detector ranged from 2 to 2.5 KeV at 1332 KeV of ^{60}Co. Aluminum was detected in lung tissue at levels of 10 to 100 ppm (wet weight). Additional trace elements identified in lung tissues included cadmium, chromium, copper, mercury, manganese, rubidium, antimony, selenium, titanium, vanadium, and zinc (*47*). Neutron activation has also been used to label asbestos fibers before administration to experimental animals and to subsequently determine the percent deposition, routes of clearance, as well as the rates of clearance of asbestos from the lower respiratory tract (*70–72*). Similar techniques have been used to study the *in vivo* solubility of certain trace elements (iron, cobalt, chromium, and scandium) associated with chrysotile asbestos (*73*). Topping and associates (*74*) used neutron activation labeling of asbestos to demonstrate the persistence of chrysotile over a 16-week period in rat heterotopic tracheal grafts in a study of effects of asbestos fibers on tracheal mucosa.

Neutron activation, like atomic absorption, is a bulk analytical technique. Its advantages include a high degree of sensitivity for many elements of interest in pulmonary toxicology (Table 2), and relative simplicity of the technique. In addition, the technique is nondestructive and has simultaneous multi-element analytic capabilities. Disadvantages inlcude the requirement for access to an atomic reactor, biological hazards associated with dealing with radioactive materials and necessary safety precautions, and the relative insensitivity of the technique for silicon (Table 2), an element of

interest in pulmonary toxicology and inorganic dust analysis.

Other Techniques

It is beyond the scope of this review to cover all of the newer analytical techniques with potential applications to pulmonary toxicology. General reviews and discussions of applicability to the field of pulmonary toxicology are available for other techniques not included in this review, such as electron spectroscopy for chemical analysis (*6,7*), acoustic microscopy (*75–78*), X-ray projection microscopy (*79,80*), laser Raman and micro-Raman spectroscopy (*81–86*) and other trace analytical techniques not included in the previous section (*69,87,88*).

Comment

The technological revolution of the past decade has made available a wide variety of techniques which may be applied to many types of samples and to the investigation of a great number of bioenvironmental problems. Many of the principles underlying the techniques are not in themselves new and have been available to physicists and chemists for some time. The technological advances, however, have enabled these analytical principles to be applied to minute samples and even to individual submicron particles or single cells with quantitative results. It has been the purpose of this chapter to discuss some of these principles and techniques, the basic components of the instrumentation, and the ways in which these methods have been or can be applied to problems in pulmonary toxicology. The relative advantages and disadvantages of each method have also been briefly reviewed. There appears to be tremendous potential application of these techniques in toxicologic and environmental research.

The advances in sample preparative techniques have been of critical importance to the application of these methodologies to bioenvironmental analysis (*89*). Some notes on preparative techniques have been included in the discussions of the individual methods; however, it is appropriate to make a few additional comments here. Analysis of electrolytes and soluble trace elements in tissues requires special precautions in sample preparation to prevent rearrangement or loss of the elements of interest, particularly when it is desirable to determine subcellular localization or intracellular mechanisms of toxicity. Rapid freezing of the tissue followed by freeze-drying and microprobe analysis minimizes loss of electrolytes or soluble trace elements such as arsenic, lead or cadmium (*38,90*). Methods have been described for preparation of cell monolayers as well as centrifuged pellets of cells, including for the latter frozen thin sections (cryoultramicrotomy) and freeze-substitution techniques (*91*). For many of these techniques, the preservation of cellular architecture and detail is surprisingly good (Fig. 10). Finally, methods have also been described whereby a paraffin-embedded, hematoxylin and eosin stained tissue section can be transferred to a scanning electron microscope stub for microanalyses of various types, permitting precise investigation of an individual particle or structure (e.g., a granuloma or foreign body crystalline material) identified by light microscopy (*92*).

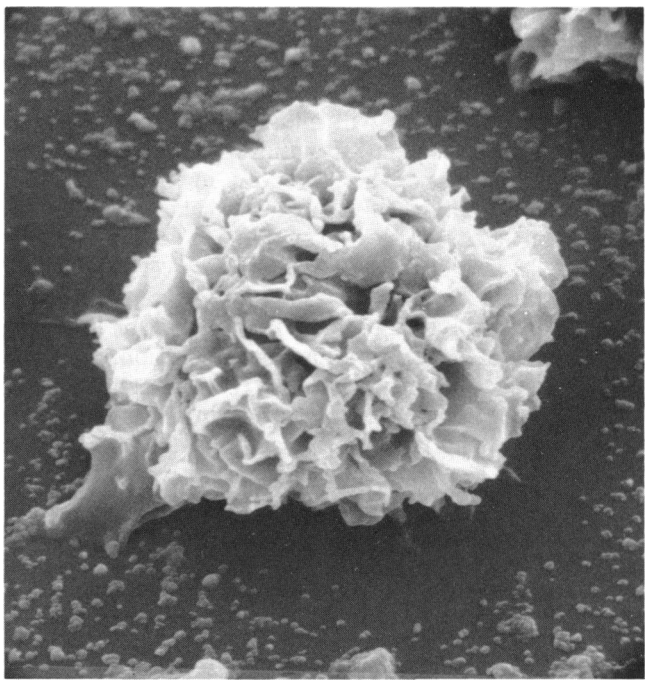

FIGURE 10. Scanning electron micrograph of a freeze-fixed, freeze-dried rabbit alveolar macrophage. Surface ruffles are well preserved. ×3890.

Sample preparation is equally important in the choice of a bulk analytical technique for trace analysis of tissue or environmental materials. Two of the conventional techniques listed in Table 2, i.e., atomic absorption and inductively coupled plasma–atomic emission spectroscopies, require that the sample be in a solution form for analysis, whereas the other two techniques, i.e., neutron activation and proton induced X-ray emission analyses, may be performed on solid (e.g., tissue) specimens. However, hybrid techniques employing a separate vaporization/atomization stage (e.g., laser) are rapidly evolving to permit direct solids analysis by AA or ICP techniques. Similarly, it should be noted that the detection limits listed in Table 2 are for optimal conditions—a situation which is rarely attainable for biological samples. Hence, these detection limits should serve merely as guidelines, and the sensitivity is reduced for many elements by matrix effects, interelement interferences, or loss of the elements of interest during extraction and dissolution. Also, the more steps involved in sample preparation, the greater the risk of introduction of contaminants. All of these factors must be considered in choosing an appropriate analytical technique for the investigational problem at hand. In addition, the trade-offs between trace analysis and

microanalysis, as emphasized by Larrabee (7) must be kept in mind by an investigator wishing to use one or more of the techniques described in this chapter to approach a problem in pulmonary toxicology.

In summary, each of the techniques discussed has its own limitations, and frequently it is to the researcher's advantage to use a combination of techniques to solve an analytical problem. For example, energy dispersive X-ray analysis may be used in combination with X-ray diffraction or selected area electron diffraction to obtain both elemental composition and crystalline structural information on a particular sample. Similarly, TRIX may be used in combination with back-scattered electron imaging, scanning electron microscopy, and energy dispersive X-ray analysis to identify, locate, and analyze inorganic particles in an organic matrix. Laser, ion, and Auger microprobe techniques are useful analytical adjuncts to energy dispersive X-ray microanalysis for the detection and imaging of elements and/or isotopes beyond the sensitivity limits of the latter technique. It is likely that such combinations of analytical approaches will be increasingly applied to many problems in pulmonary toxicology in the coming decade, and the results will undoubtedly stimulate further investigations and suggest even newer approaches to the complexities of bioenvironmental interactions.

This work was supported in part by the Diagnostic Electron Microscopy Laboratory of the Veterans Administration Medical Center, Durham, NC, by NIEHS Grant Nos. ESHL01581 and ESO7031, and by E.P.A. Grant Nos. R805460–2 and CR807560–01. Jessie Calder and Don Powell provided assistance with the photography and illustrations, respectively. Walter Fennell and Elena Whitted prepared the thin sections, and Martha Farmer provided assistance with the secondary ion mass spectrometry experiments.

REFERENCES

1. Beaman, D. R., and Isasi, J. A. Electron Beam Microanalysis, American Society for Testing and Materials, ASTM Publication 506, Philadelphia, PA, 1972.
2. Ingram, P., and Shelburne, J. D. Total rate imaging with X-rays (TRIX)—a novel form of X-ray microscopy in SEM and its application to biological specimens. In: Scanning Electron Microscopy, Vol. II. SEM Inc., AMF O'Hare, IL, 1980, pp. 285–296.
3. Legge, G. J. F., and Hammond, I. Total quantitative recording of elemental maps and spectra with a scanning microprobe. J. Micros. 117: 201–210 (1979).
4. Chattarji, D. The Theory of Auger Transitions. Academic Press, London, 1976.
5. Harris, L. A. Analysis of materials by electron-excited Auger electrons. J. Appl. Phys. 39: 1419–1427 (1968).
6. Keyser, T. R., Natusch, D. F. S., Evans, C. A., Jr., and Linton, R. W. Characterizing the surfaces of environmental particles. Environ. Sci. Technol. 12: 768–773 (1978).
7. Larrabee, G. B. The characterization of solid surfaces. In: Scanning Electron Microscopy, Vol. I. IIT Research Inst., Chicago, 1977, pp. 639–650.
8. Linton, R. W. Surface microanalytical techniques for chemical characterization of airborne particulates. In: Monitoring Toxic Substances, ACS Symposium Series, 94 (D. Schuetzle, Ed.), Washington, DC, 1979, pp. 137–159.
9. Palmberg, P. W., Bohn, G. K., and Tracy, J. C. High sensitivity Auger electron spectrometer. Appl. Phys. Letters 15: 254–255 (1969).
10. Isaacson, M. All you might want to know about ELS (but are afraid to ask): a tutorial. In: Scanning Electron Microscopy, Vol. I. SEM Inc., AMF O'Hare, IL, 1978, pp. 763–776.
11. Galle, P., Berry, J. P., and LeFevre, R. Microanalysis in biology and medicine: a review of results obtained with three microanalytical methods. In: Scanning Electron Microscopy, Vol. II (O. Johari and R. P. Becker, Eds.), SEM Inc., AMF O'Hare, IL, 1979, pp. 703–710.
12. Silcox, J. Inelastic electron scattering as an analytical tool. In: Scanning Electron Microscopy, IIT Research Inst., Chicago, IL, 1977, pp. 393–400.
13. Shelburne, J. D., Ingram, P., Hawkins, H. K., and Waters, M. D. X-ray mapping of lysosomal inclusions. In: Scanning Electron Microscopy, Vol. III (O. Johari and R. P. Becker, Eds.), IIT Research Inst., Chicago, 1976, pp. 485–500.
14. Abraham, J. L., Rossi, R., Marquez, N., and Wagner, R. M. Ion microprobe mass analysis of beryllium *in situ* in human lung: preliminary results. In: Scanning Electron Microscopy, Vol. III. IIT Research Inst., Chicago, 1976, pp. 501–506.
15. Liebl, H. SIMS instrumentation and imaging techniques. In: Scanning Electron Microscopy, Vol. III. SEM Inc., AMF O'Hare, IL, 1980, pp. 79–90.
16. Linton, R. W., Walker, S. R., DeVries, C. R., Ingram, P., and Shelburne, J. D. Ion microanalysis of cells. In: Scanning Electron Microscopy, Vol. II. SEM Inc., AMF O'Hare, IL, 1980, pp. 583–596.
17. Storms, H. A., Brown, K. F., and Stein, J. D. Evaluation of a cesium positive ion source for secondary ion mass spectrometry. Anal. Chem. 49: 2023–2030 (1977).
18. Kaufman, R., Hillenkamp, F., Wechsung, R., Heinen, H. J., and Schürman, M. Laser microprobe mass analysis: achievements and aspects. In: Scanning Electron Microscopy, Vol. II. SEM Inc., AMF O'Hare, IL 1979, pp. 279–290.
19. Kaufman, R., and Wieser, P. Laser microprobe mass analysis (LAMMA) in particle analysis. In: Characterization of Particles. NBS Spec Pub. 533, Natl. Bur. Standards, Washington, DC, 1980, pp. 199–223.
20. Kaufman, R., Wieser, P., and Wurster, R. Application of the laser microprobe mass analyzer LAMMA in aerosol research. In: Scanning Electron Microscopy, Vol. II. SEM Inc., AMF O'Hare, IL, 1980, pp. 607–622.
21. Schmidt, P. F., Fromme, H. G., and Pfefferkorn, G. LAMMA-investigations of biological and medical specimens. In: Scanning Electron Microscopy, Vol. II. SEM Inc., AMF O'Hare, IL, 1980, pp. 623–634.
22. Wechsung, R., Hillenkamp, F., Kaufman, R., Nitsche, R., and Vogt, H. LAMMA—a new laser microprobe mass analyzer. In: Scanning Electron Microscopy, Vol. I. SEM Inc., AMF O'Hare, IL, 1978, 611–620.
23. Beeston, B. E. P. An introduction to electron diffraction. In: Electron Diffraction and Optical Diffraction Techniques (A. M. Glauert, Ed.), North-Holland, Amsterdam, 1972.
24. Berry, J. P., Henoc, P., Galle, P., and Pariente, R. Pulmonary mineral dust: a study of ninety patients by electron microscopy, electron microanalysis and electron microdiffraction. Am. J. Pathol. 83: 427–456 (1976).
25. Brody, A., and Craighead, J. Cytoplasmic inclusions in pulmonary macrophages of cigarette smokers. Lab. Invest. 32: 125–132 (1975).
26. Churg, A., and Warnock, M. L. Analysis of the cores of ferruginous (asbestos) bodies from the general population. I. Patients with and without lung cancer. Lab. Invest. 37: 280–286 (1977).
27. Churg, A., Warnock, M. L., and Green, N. Analysis of the cores of ferruginous (asbestos) bodies from the general population. II. True asbestos bodies and pseudoasbestos bodies. Lab. Invest. 40: 31–38 (1979).
28. Churg, A., and Warnock, M. L. Analysis of the cores of ferruginous (asbestos) bodies from the general population. III.

Patients with environmental exposure. Lab. Invest. 40: 622–626 (1979).
29. Roggli, V. L., Greenberg, S. D., Seitzman, L. H., McGavran, M. H., Hurst, G. A., Spivey, C. G., Nelson, K. G., and Hieger, L. R. Pulmonary fibrosis, carcinoma, and ferruginous body counts in amosite asbestos workers: a study of six cases. Am. J. Clin. Pathol. 73: 496–503 (1980).
30. Barrow, R. E. X-ray diffraction analysis of quartz in lung tissue. Tex. Rep. Biol. Med. 32: 441–448 (1974).
31. Bragg, S. L. The Development of X-ray Analysis (D. C. Phillips and H. Lipson, Eds.), G. Bell and Sons, London, 1975.
32. Lange, B. A., and Haartz, J. C. Determination of microgram quantities of asbestos by X-ray diffraction: chrysotile in thin dust layers of matrix material. Anal. Chem. 51: 520–525 (1979).
33. McCrone, W. C., and Delly, J. G. X-ray diffraction. In: The Particle Atlas, Volume I, 2nd ed. Ann Arbor Science Publishers, Ann Arbor, MI, 1973, pp. 119–129.
34. Mastin, J. P., Furbish, W. J., Gutknecht, W. F., Ingram, P., and Shelburne, J. D. Respirable inorganic particulates in cigarette smoke (abstr.). Paper presented before The Clay Minerals Society 17th Annual Meeting and 29th Annual Clay Minerals Conference, Baylor University, Waco, Texas, Oct. 5–9, 1980.
35. Middleman, L. M., Geller, J. D. Trace element analysis using X-ray excitation with an energy dispersive spectrometer on a scanning electron microscope. In: Scanning Electron Microscopy, Vol. I, IIT Research Inst., Chicago, 1976, pp. 171–178.
36. Bosch, F., Goresy, A. E., Martin, B., Povh, B., Nobiling, R., Schwalm, D., and Traxel, K. The proton microprobe: a powerful tool for nondestructive trace element analysis. Science 199: 765–768 (1978).
37. Walter, R. L., Willis, R. D., Gutknecht, W. F., and Joyce, J. M. Analysis of biological, clinical, and environmental samples using proton-induced X-ray emission. Anal. Chem. 46: 843–855 (1977).
38. Feussner, J. R., Shelburne, J. D., Bredehoeft, S., and Cohen, H. J. Arsenic-induced bone marrow toxicity: ultrastructural and electron-probe analysis. Blood 53: 820–827 (1979).
39. Robinson, J. W. Atomic Absorption Spectroscopy, Marcel Dekker, New York, 1966.
40. Strobel, H. A. Chemical Instrumentation: A Systematic Approach to Instrumental Analysis, 2nd ed. Addison-Wesley, Reading, MA, 1973, pp. 390–418.
41. Toda, W., Lux, J., and Van Loon, J. C. Determination of aluminum in solutions from gel filtration chromatography of human serum by electrothermal atomic absorption spectrometry. Anal. Letters 13(B13): 1105–1113 (1980).
42. Fassel, V. A. Simultaneous or sequential determination of the elements at all concentration levels—the renaissance of an old approach. Anal. Chem. 51: 1291A–1308A (1979).
43. Bradbury, H. Biological sample analysis with ICAP spectroscopy. Jarrell-Ash Plasma Newsletter 1: 3–4 (1978).
44. Ward, A. F., and Marciello, L. Analysis of energy resources by ICAP spectroscopy, Part I: Coal fly ash and coal. Jarrell-Ash Plasma Newsletter 1: 10–11 (1978).
45. Kay, M. A., McKown, D. M., Gray, D. H., Eichor, M. E., and Vogt, J. R. Neutron activation analysis in environmental chemistry. Amer. Lab. 5: 39–48 (1973).
46. Niom, D. B., Nordberg, G. F., Wester, P. O., and Bivered, B. Accumulation of heavy metals in tissues of industrially exposed workers. In: Nuclear Activation Techniques in the Life Sciences. Proceedings, International Symposium on Nuclear Activation Techniques in the Life Sciences, International Atomic Energy Agency, Vienna, 1979, pp. 643–655.
47. Yukawa, M., Suzuki-Yasumoto, M., Amano, K., and Terai, M. Distribution of trace elements in the human body determined by neutron activation analysis. Arch. Environ. Health 35: 36–44 (1980).
48. Brody, A. R. Inhaled particles in human disease and animal models: use of electron beam instrumentation. Environ. Health Perspect. 56: 149–162 (1984).
49. Abraham, J. L. Recent advances in pneumoconiosis: the pathologists' role in etiologic diagnosis. In: The Lung (IAP Monograph 19), Williams and Wilkins Co., Baltimore, 1978, pp. 96–137.
50. Shelburne, J. D., Gutknecht, W. F., Wilder, D. R., Ingram, P., and Hawkins, H. K. Respirable silicon-positive particles in cigarette smoke. Federation Proc. 38: 1155 (1979).
51. Bodner, S. M., Spicer, S. S., Ingram, P., Spock, A., and Shelburne, J. D. Carbohydrate histochemistry of surface epithelium of rat trachea: backscatter and X-ray imaging. In: Scanning Electron Microscopy, Vol. II. SEM Inc., AMF O'Hare, IL, 1981, pp. 105–114, 104.
52. Lynn, W. S., Kylstra, J. A., Sahu, S. C., Tainer, J., Shelburne, J. D., Pratt, P. C., Gutknecht, W. F., Shaw, R., and Ingram, P. Investigation of black bronchoalveolar human lavage fluid. Chest 72: 483–488 (1977).
53. ASTM Index to the Powder Diffraction File, American Society for Testing and Materials, Philadelphia.
54. Dean, J. A., and Rains, T. C. Flame Emission and Atomic Absorption Spectrometry, Vol. 3. Marcel Dekker, New York, 1975.
55. Fuller, C. W. Electrothermal Atomization for Atomic Absorption Spectrometry. Chemical Society, London, 1977.
56. Jarrell-Ash Division, Fisher Scientific Co., Bulletin No. 434 A, Waltham, MA, 1978.
57. Slavin, M. Atomic Absorption Spectroscopy. John Wiley and Sons, New York, 1978.
58. Stika, K. M., and Morrison, G. H. Analytical methods for the mineral content of human tissues. Fed. Proc. 40: 2115–2119 (1981).
59. Willis, R. D. Proton induced X-ray emission (PIXE) and applications to elemental analysis. Ph.D. Thesis, Duke University, Durham, NC, 1977, pp. 237–248.
60. Walter, R. L., Willis, R. D., Gutknecht, W. F., and Shaw, R. W. The application of proton-induced X-ray emission to bioenvironmental analyses. Nucl. Instr. Meth. 142: 181–197 (1977).
61. Bartsch, P., Collignon, A., Weber, G., Robaye, G., Delbrouck, J. M., Roelandts, I., and Yujie, J. Distribution of metals in human lung: analysis by particle induced X-ray emission. Arch. Environ. Health 37: 111–117 (1982).
62. Czanderna, A. W., Miller, A. C., and Helbig, H. F. Surface analysis from scattered and sputtered ions. In: Scanning Electron Microscopy, Vol. I. SEM Inc., AMF O'Hare, IL, 1978, pp. 259–272.
63. Fiermans, L., Vernik, J., and Dekeyser, W. (Eds.). Electron and Ion Spectroscopy of Solids. Plenum Press, New York, 1978.
64. Spurr, A. R. Applications of SIMS in biology and medicine. Scanning 3: 97–110 (1980).
65. Thomas, J. P., and Cachard, A. (Eds.). Materials Characterization Using Ion Beams. Plenum Press, New York, 1978.
66. Furman, A. K., and Morrison, G. H. Direct digitization system for quantification in ion microscopy. Anal. Chem. 52: 2305–2310 (1980).
67. Johnstone, R. A. W., and Plimmer, J. R. Constituents of tobacco and tobacco smoke. Chem. Rev. 59: 885–936 (1959).
68. Larson, P. S., and Siluette, H. Tobacco—Experimental and Chemical Studies, Supplement III. Williams and Wilkins, Baltimore, 1975, pp. 294–295.
69. Winefordner, J. D. Trace Analysis: Spectroscopic Methods for Elements. John Wiley and Sons, New York, 1976.
70. Evans, J. C., Evans, R. J., Holmes, A., Hounam, R. F., Jones, D. M., Morgan, A., and Walsh, M. Studies on the deposition of inhaled fibrous material in the respiratory tract of the rat and its subsequent clearance using radioactive tracer techniques: I. UICC crocidolite asbestos. Environ. Res. 6: 180–201 (1973).
71. Morgan, A., Evans, J. C., Evans, R. J., Hounam, R. F., Holmes, A., and Doyle, S. G. Studies on the deposition of inhaled fibrous material in the respiratory tract of the rat and its subsequent clearance using radioactive tracer techniques. II. Deposition of the UICC standard reference samples of asbestos. Environ. Res. 10: 196–207 (1975).
72. Morgan, A., Talbot, R. J., and Holmes, A. Significance of fibre

length in the clearance of asbestos fibres from the lung. Brit. J. Ind. Med. 35: 146–153 (1978).
73. Morgan, A., Holmes, A., and Gold, C. Studies of the solubility of constituents of chrysotile asbestos *in vivo* using radioactive tracer techniques. Environ. Res. 4: 558–570 (1971).
74. Topping, D. C., Nettesheim, P., and Martin, D. H. Toxic and tumorigenic effects of asbestos on tracheal mucosa. J. Environ. Pathol. Toxicol. 3: 261–275 (1980).
75. Cargill, G. S., III. Ultrasonic imaging in scanning electron microscopy. Nature 286: 691–693 (1980).
76. Maugh, T. H., II. Acoustic microscopy: a new window to the world of the small. Science 201: 1110–1114 (1978).
77. Quate, C. F. The acoustic microscope. Sci. American. 241: 62–70 (1979).
78. Rochow, T. G., and Rochow, E. G. Acoustic microscopy. In: An Introduction to Microscopy by Means of Light, Electrons, X-rays, or Ultrasound. Plenum Press, New York, 1978, pp. 319–351.
79. Horn, H. R. F., and Waltinger, H. G. How to obtain and use X-ray projection microscopy in the SEM. Scanning 1: 100–108 (1978).
80. Parsons, D. F. Ultrasoft X-Ray Microscopy: Its Application to Biological and Physcial Sciences. New York Academy of Sciences, New York, 1980.
81. Abraham, J. L., and Etz, E. S. Molecular microanalysis of pathological specimens *in situ* with a laser-Raman microprobe. Science 206: 716–718 (1979).
82. Adar, F. Applications of the molecular optical laser examiner —some examples. In: Scanning Electron Microscopy, Vol. I (O. Johari and R. P. Becker, Eds.), SEM Inc., AMF O'Hare, IL, 1979, pp. 83–92.
83. Blaha, J. J., Etz, E. S., and Cunningham, W. C. Molecular analysis of microscopic samples with a Raman microprobe: applications to particle characterization. In: Scanning Electron Microscopy, Vol. I. (O. Johari and R. P. Becker, Eds.), SEM Inc., AMF O'Hare, IL, 1979, pp. 93–102.
84. Etz, E. S. Raman microprobe analysis: principles and applications. In: Scanning Electron Microscopy, Vol. I (O. Johari and R. P. Becker, Eds.), SEM Inc., AMF O'Hare, IL, 1979, pp. 67–82.
85. Gardiner, D. J. Raman spectrometry. Anal. Chem. 52: 96R–100R (1980).
86. Tobin, M. D. Laser Raman Spectroscopy. Wiley-Interscience, New York, 1971.
87. Horwitz, W. Official Methods of Analysis of the Association of Official Analytical Chemists. Association of Official Analytical Chemists, Washington, DC, 1980.
88. Meites, L. Handbook of Analytical Chemistry. McGraw-Hill, New York, 1963.
89. Walker, S. R., and Shelburne, J. D. Preparative techniques for scanning electron microscopy. In: Methods for Studying Mononuclear Phagocytes (D. O. Adams, P. J. Edelson, and H. S. Koren, Eds.), Academic Press, New York, 1981, pp. 403–412.
90. Bell, S. W., Masters, S. K., Ingram, P., Waters, M., and Shelburne, J. D. Ultrastructure and X-ray microanalysis of macrophages exposed to cadmium chloride. In: Scanning Electron Microscopy, Vol. III. SEM Inc., AMF O'Hare, IL, 1979, pp. 111–121.
91. Masters, S. K., Bell, S. W., Ingram, P., Adams, D. O., and Shelburne, J. D. Preparative techniques for freezing and freeze-sectioning macrophages for energy dispersive X-ray microanalysis. In: Scanning Electron Microscopy, Vol. III (O. Johari and R. P. Becker, Eds.), SEM Inc., AMF O'Hare, IL, 1979, pp. 97–110, 122.
92. Pickett, J. P., Ingram, P., and Shelburne, J. D. Identification of inorganic particulates in a single histologic section using both light microscopy and X-ray microprobe analysis. J. Histotechnol. 3: 155–158 (1980).